ASSESSING THE POTENTIAL CONTRIBUTION OF LATEX FROM RUBBER (HEVEA BRASILIENSIS) PLANTATIONS AS A CARBON SINK

EKOW NYAMEKYE TAWIAH
March, 2017

SUPERVISORS:
Ir. L.M. van Leeuwen - de Leeuw (Louise)
Ing. G. Ashiagbor (George)
Dr. I.C. van Duren (Iris)

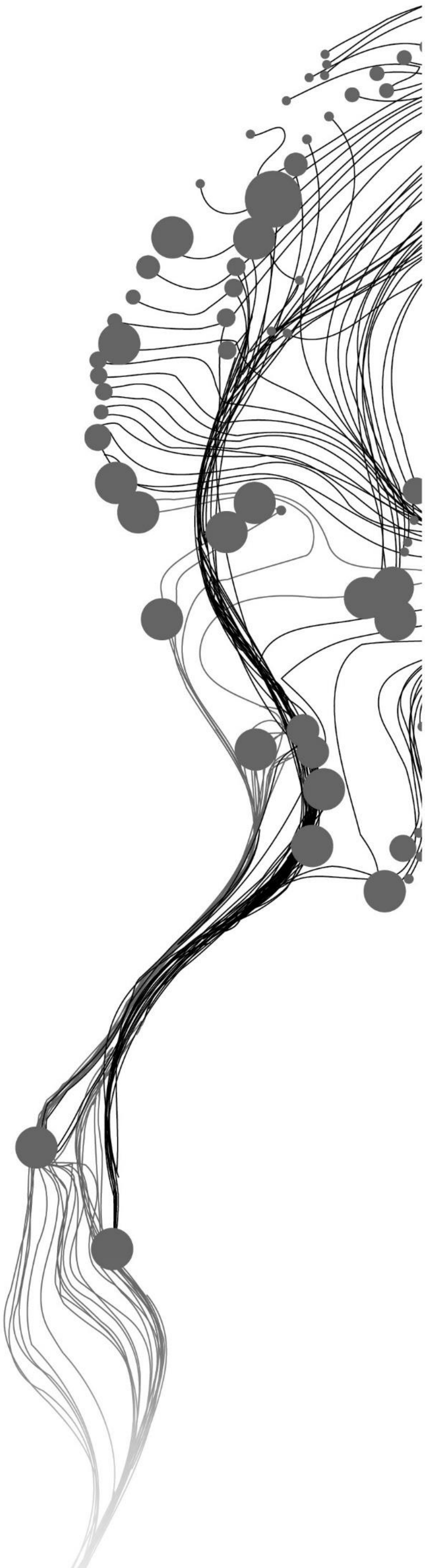

ASSESSING THE POTENTIAL CONTRIBUTION OF LATEX FROM RUBBER (HEVEA BRASILIENSIS) PLANTATIONS AS A CARBON SINK

EKOW NYAMEKYE TAWIAH
Enschede, The Netherlands, March, 2017
Kumasi, Ghana, March, 2017

Thesis submitted to the Faculty of Geo-Information Science and Earth Observation of the University of Twente in partial fulfilment of the requirements for the degree of Master of Science in Geo-information Science and Earth Observation.
Specialization: Natural Resources Management

SUPERVISORS:
Ir. L.M. van Leeuwen - de Leeuw (Louise)
Ing. G. Ashiagbor (George)
Dr. I.C. van Duren (Iris)

THESIS ASSESSMENT BOARD:
Prof. Dr. A. D. Nelson (Chair)
Dr. W. A. Asante (Internal Examiner, KNUST)
Dr. B. Kumi-Boateng (External Examiner, UMaT)

ABSTRACT

The attention and focus of scientific and public studies about the benefits of rubber (Hevea brasiliensis) in recent times have not only been on the socio-economic importance but also environmental benefits of carbon sequestration. Sequestered carbon is stored in carbon pools such as aboveground biomass, belowground biomass, soil, dead wood and litter, however, the contribution of latex to carbon sequestration is overlooked. This study employed tier 3 allometric equations to compute aboveground carbon (stem and foliage) and below ground carbon relative to the use of the dry rubber content fraction to compute the carbon content in latex. Additionally, object based image analysis was performed on google earth data to explore the prediction of rubber tree diameter at breast height from segmented google earth image into tree crowns. Across different age categorisations of 9 years to 22 years, it was observed that carbon sequestered by the latex ranged from 2.08 t C ha-1 to 17.36 t C ha-1. This means that the carbon from latex increases with age since tapping intensity of the latex increases as the rubber trees grow older. There were significant differences observed in the latex carbon from the different age classes. Latex carbon from the age stands above 20 years were significantly higher than carbon from latex computed for age stands that were younger than 20 years. Aboveground carbon computed for the different ages of 9 to 20 years was in the range of 38.08 t C ha-1 to 126.6 t C ha-1 whereas belowground carbon ranged from 5.77 t C ha-1 to 12.47 t C ha-1. Comparing the three carbon pools, aboveground carbon had a significantly higher carbon sequestration capacity with an effect size of 75% whilst sequestered carbon by both the belowground carbon pool and the latex carbon pool had no significant differences between then with a recorded effect size of 4% each. The root to shoot ratio decreased as the ages of the rubber plantation increased. Although the carbon sequestered by the belowground pool was higher than the carbon in the latex, the opposite occurs as the age of the plantation increases. Carbon from the latex increases about 3% more than the belowground carbon as the plantation age increases. The carbon found in the latex is no different from the carbon contained in the belowground pool, thus, latex is equally important for carbon accounting for rubber plantations. Reference polygons from google earth were 190 with 102 polygons having a one to one matching. Over-segmentation and under-segmentation resulted in 0.43 and 0.32 respectively with overall accuracy observed as 62%. Linear, quadratic and cubic models poorly predicted tree diameter as the recorded correlation coefficients were 0.119, 0.370 and 0.373 respectively. The inability to predict tree diameter accurately could be attributed to the factor that, spectral quality of the google earth imagery is low, especially as the near infrared band which is necessary for vegetation analysis is absent.

Keywords: Carbon Pool, Latex, Aboveground, Belowground, Rubber, Carbon, Segmentation

ACKNOWLEDGEMENTS

The sun does not shine forever, neither does the rain fall forever. To every beginning there is an end and in every end is embedded a new beginning. My greatest thanks goes to the "Giver of Life" – God Almighty for His consistent grace, sustenance and sufficiency.

Further appreciation goes to my boss Mr. David T. Addo for nominating me for the Netherlands Fellowship Programme (NFP) and to NUFFIC for granting the fellowship to enable me successfully go through the study.

I wish to acknowledge Ing. George Ashiagbor for his support through the application process, and my deepest gratitude goes to my supervisors Ir. Louise M. van Leeuwen - de Leeuw, Ing. George Ashiagbor, Dr. Iris C. van Duren and Dr. Winston A. Asante for their timely responses and feedback throughout the thesis preparation. The constructive and thought provoking comments from my supervisors gave me great insights.

I am thankful to the staff of the Department of Wildlife and Range Management – KNUST and the staff of ITC for their continued support in developing the best environments to enable me go through the study successfully.

The support from Ghana Rubber Estate Limited (GREL) in terms of staff and data cannot go unnoticed, sincerest appreciation to Mr. Gregory Mensah and Mr. Benjamin Bentil.

My sincerest gratitude goes to my family, especially to my parents for their prayers, encouragement and moral supports. Your presence has a great value for me. You have always special place in my heart. God bless you.

I further wish to acknowledge support from my siblings Felix Fordjour, Enoch A.B.P. Tawiah, Obed E. Tawiah and Pauline M. Nkrumah.

Last but not least to my best friends Dorothy Danso, Sylvia Donk, Ollette Lawrence, Frederick A. Ampah, Jefferson Okojie, Marijana Demajo and my colleagues Kelvin Joseph Kamnde and Emma Baah Agyapong and all the ITC colleagues, I remain indebted to you all for your support.

TABLE OF CONTENTS

LIST OF FIGURES

LIST OF TABLES

LIST OF EQUATIONS

LIST OF APPENDICES

LIST OF ABBREVIATIONS

AGB	Aboveground Biomass
AGC	Aboveground Carbon
AR CDM	Afforestation and Reforestation Clean Development Mechanism
BGB	Belowground Biomass
BGC	Belowground Carbon
Bha	Billion hectares
C170	Circumference at 170cm
CDM	Clean Development Mechanism
CF	Conversion factor
COP	Conference of parties
CPA	Crown Projection Area
DBH	Diameter at Breast Height
DBH170	Diameter at Breast Height at 170cm
DF	Default factor
DRC	Dry Rubber Content
ESP	Estimation of Scale Parameter
FOTO	Fourier Textural Ordination
GDP	Gross Domestic Product
GPS	Global Positioning System
GREL	Ghana Rubber Estate Limited
LV	Local Variance
MAPE	Mean Absolute Percentage Error
Mha	Million hectares
OBIA	Object Based Image Segmentation
REDD/ REDD+	Reduced Emissions from Deforestation and Forest Degradation
RGB	Red, Green and Blue
ROC-LV	Rate of Change of Local Variance
RMSE	Root Mean Square Error
SOC	Soil Organic Carbon
TSC	Total Solid Content
VHR	Very High Resolution

1. INTRODUCTION

1.1. Background

Socio-economic development is desirable across various cultures hence world organisations, countries and individuals channel their efforts towards attaining goals of development driven by industrialization. The drive for development through industrialization has led to increased emissions of greenhouse gases (GHGs) into the atmosphere (IPCC, 2014) which is warming our globe resulting in global climate change. Prominent among the GHGs is the substantial increase in carbon emissions from sources such as burning of fossil fuels, loss of forests among other anthropogenic developmental activities (Ingvaldsen & Gulla, 2015). These GHGs including carbon act like a protective roof to prevent longwave solar radiation from escaping the earth's atmosphere thereby causing the greenhouse effect of global warming (Figure 1).

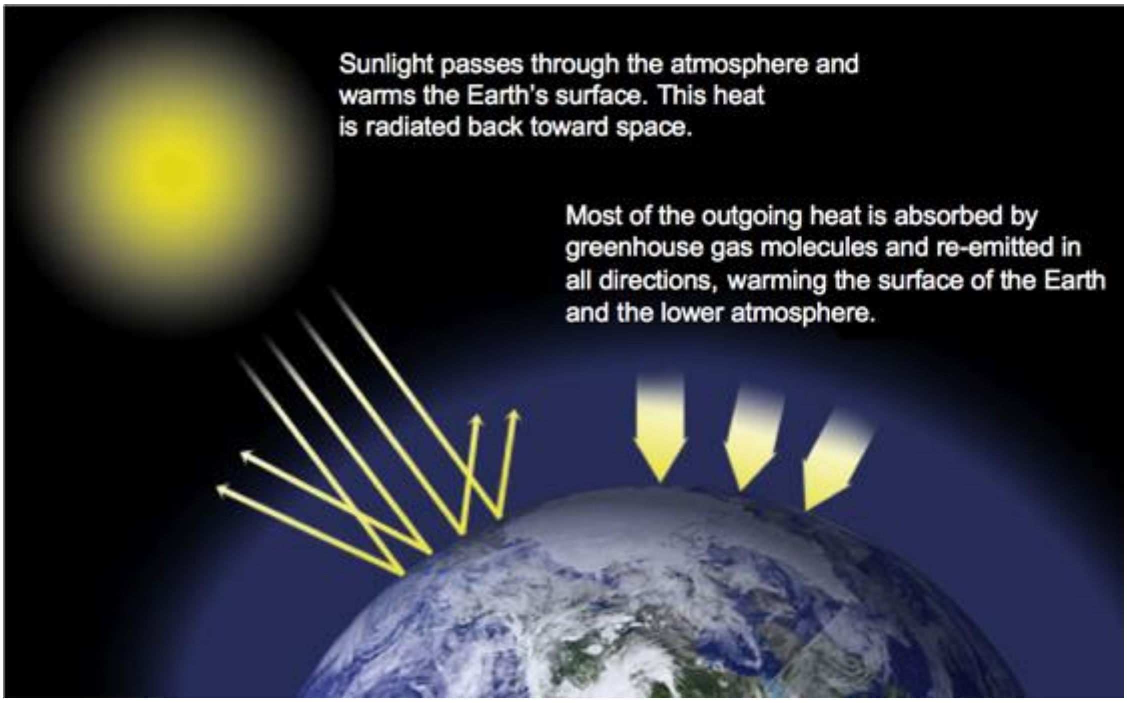

Figure 1: Greenhouse effect caused by emissions from GHGs

Source: (NASA, n.d.)

The continuous trend of increasing carbon concentration in the atmosphere is a major concern as the effects of climate change and global warming imminently dawns on humanity, yet we cannot halt the drive for development and industrialization.

Innovative mitigation strategies have been designed to help deal with this trend of rising carbon emissions such as Reduced Emissions from Deforestation and Forest Degradation (REDD) and later REDD+ which included conservation, maintaining and enhancing carbon stocks (Srivastava, 2008). The REDD+ mechanism is a United Nations programme aimed at offering financial incentives towards the motivation of countries to target the reduction of deforestation and its associated carbon emissions by conservation, sustainable management and enhancement of carbon stocks (UN-REDD, 2013; UNFCCC, 2016). Another dimension to climate change mitigation strategies is the Clean Development Mechanism (CDM) which encourages projects aimed at carbon emissions reduction in developing countries for carbon emissions trading in the form of certified emission reduction (CER) credits (UNFCCC, 1997). A further boost for carbon financing incentives is the Afforestation Reforestation Clean Development Mechanism (AR CDM) under the CDM programme which encourages interventions that lead to additional increase in carbon stocks which ordinarily would not have experienced any increase (UNFCCC, 2015). These include improving natural forests or planted forests which are also considered for carbon financing under AR CDM, and is also in line with the 9th session of the Conference of Parties agreement in Milan, Italy (Watson, 2009). All these incentives and interventions aim to develop green vegetation, especially forests and planted forests alike, to sequester carbon from the atmosphere and to prevent further losses of the earth's green cover.

Tree crop plantations have demonstrated the ability to help mitigate global challenges in terms of climate change, clothing, shelter as well as industrialization among many others (Mbabazi, 2011). Therefore, there is the increasing global trend of this tree crop plantation establishment for different varieties of trees. Some established plantations include teak, acacia, cocoa, eucalyptus, rubber and many others (Yuen, Ziegler, Webb & Ryan, 2013)

Rubber (*Hevea brasiliensis*) on large scale production are accounted for as planted forests (Egbe, Tabot, Fonge & Bechem, 2012) which could contribute to development by financial gains and carbon emissions reduction. Rubber plantations qualify for carbon financing under AR CDM with a long lifespan of over 25 years and they also contribute to socio-economic well-being of humanity (Munasinghe, Rodrigo & Gunawarden, 2014). A typical case of rubber afforestation and reforestation is in Columbia where highly degraded lands have seen rubber cultivation of 1,500 hectares (World Bank, 2005).

Hevea brasiliensis is cultivated on large-scale plantation farms purposefully for the latex it produces which is used for manufacturing gloves, catheters, vehicle tyres and many other products (Venkatachalam, Geetha, Sangeetha & Thulaseedharan, 2013). The harvested wood is an alternative to harvesting primary forests and used for furniture, housing, toys among others (FAO, 2010; Petsri, Chidthaisong, Pumijumnong & Wachrinrat, 2013). Although the harvested and processed wood may not continue to sequester carbon, it becomes a long term storage for sequestered carbon of over 3% more than instances where there is no harvesting of timber (Liu & Han, 2009).

Global massive expansion of rubber plantations has been recorded in the world's sub-tropical and tropical areas over the past 50 years (Chen et al., 2016). This rapid development of rubber plantations is recorded in Southeast-Asia, the Amazon Basin and Africa with an estimated total planted area of 10 million hectares (M ha) out of the estimated 4 billion hectares (B ha) for total world forests (FAO, 2010).

In Ghana, the production and export of rubber can be traced to the 1860s according to Dickson (1971) as cited in (Arhin, 1980). In 1962, rubber plantations in the Western Region, precisely Dixcove were 36,390 hectares, and in Abura and Subri a total of 1,989 hectares (GREL, n.d.). By 2008, rubber plantations in Abura around Agona had expanded to about 11,000 hectares (Wauters, Coudert, Grallien, Jonard & Ponette, 2008). Available statistics indicate that rubber production is a significant contributor to the economy of Ghana as together with other agricultural crops, they make up 19.5% of Gross Domestic Product (AfDB/OECD/UNDP, 2015).

The continual expansion of rubber plantations generates keen interests to further investigate its role in the environment especially carbon sequestration (Nizami et al., 2014).

The application of remote sensing for woody biomass and carbon monitoring saves time and covers vast areas hence the European Space Agency's advanced plans to launch the 'Biomass Satellite' (ESA, 2012). This technology is to facilitate the monitoring of forest biomass and enable proper management and enhancement of world forests and biomass. Remote sensing technologies may employ active sensors or passive sensors which are dependent on detecting reflected emitted electromagnetic radiation from the earth surface (Lu, 2006). Remote sensing approach presents a faster way of data collection over vast areas and is less labour intensive compared to the destructive method of tree felling. The approach of using satellite imagery to extract the biophysical properties of vegetation for biomass and carbon estimation over large areas has proved effective and efficient over time (Lu et al., 2014). This is an indirect procedure which can be validated with field measured samples of these biophysical properties. Optical imagery with Very High Resolution (VHR) of less than 5 m provide fine details which help to extract tree parameters such as the crown projected area (CPA) which forms a basis for extracting tree parameters for biomass estimation (Karna et al., 2015).

1.2. Research problem

Carbon pools that are factored into carbon estimation for rubber plantations include aboveground biomass, belowground biomass, soil organic matter, dead wood (Kongsager, Napier & Mertz, 2013). However, the omission of the latex carbon content as a carbon pool for rubber plantations makes the carbon potential assessment incomplete (Blagodatsky, Xu & Cadisch, 2016). Including latex carbon content in carbon sequestration accounting will be a more complete expression of the actual carbon sequestration potential of rubber plantations. This will help to expand the knowledge on the role of rubber plantations in sequestering carbon especially considering whether the carbon from the latex is significant enough to be considered as a carbon pool. Although the latex is harvested, the carbon in the latex is stored over longer years and not released into the atmosphere (Liu & Han, 2009). Latex has a very long shelf life with no definitely known period of degradation, therefore, carbon stored in latex and latex products will be stored for a longer time. Therefore, it is very important to complement carbon sequestration studies for rubber plantations with the knowledge of the potential contribution from latex to carbon storage.

Furthermore, carbon estimation of rubber plantations for vast areas could be tedious and cumbersome given time and financial resources. The availability of free Very High Resolution (VHR) Imagery from Google Earth could prove as a useful indirect method for carbon estimation. The application of Google Earth Imagery for the extraction of rubber tree crowns for carbon estimation has not yet been well explored.

1.3. Research objectives

The research seeks to determine the potential contribution of latex from rubber plantations as a carbon pool in relation to aboveground carbon and belowground carbon and the potential of using Google Earth Images to estimate aboveground and belowground carbon across different ages of rubber plantations.

1.3.1. Specific objectives

1. To determine the differences in carbon from latex for the different ages categories.
2. To assess the differences in carbon from latex, aboveground and belowground pools.
3. To analyze the relationship between Google Earth derived Canopy Projection Area and Diameter at Breast Height.

1.3.2. Research questions

1. How does carbon from latex differ across different age categories?
2. How significant are the differences in the contribution of latex, aboveground and belowground carbon pools to carbon sequestration?
3. How strong is the relationship between Google Earth derived Canopy Projection Area and Diameter at Breast Height?

1.3.3. Hypothesis

H_a = There is a significant difference in carbon from latex for the different age categories.

H_a = There are significant differences in contribution of latex, aboveground and belowground carbon pools to carbon sequestration.

H_a = There is a significant relationship between Google Earth derived Canopy Projection Area and Diameter at Brest Height.

2. LITERATURE REVIEW

2.1. Carbon sequestration

Carbon sequestration refers to the removal and storage of carbon from the atmosphere or sources of emission into terrestrial, oceanic and geo-sinks either by natural or deliberate means (Sundquist et al., 2008). Terrestrial carbon sinks include the vegetation cover (forests, grasslands and wetlands) and soils as depicted in Figure 2. Terrestrial carbon sinks such as forests and wetlands are key to carbon financing initiatives such as REDD+ and CDM programmes.

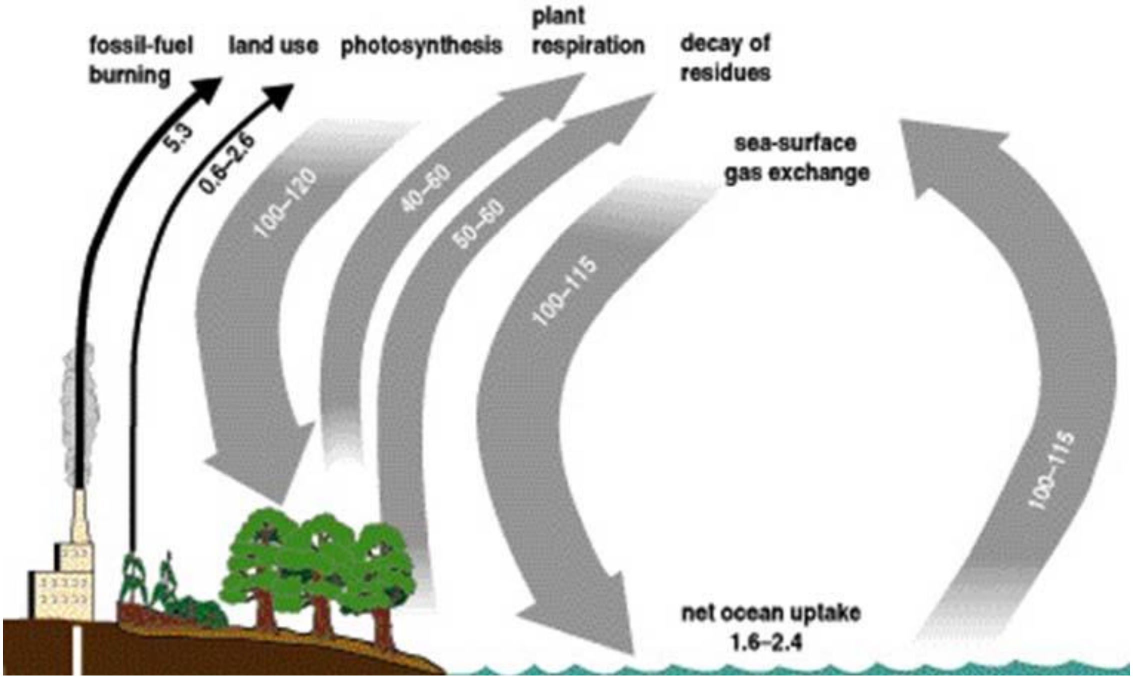

Figure 2: Carbon sequestration process

Source: (Blinn, Zamora & Taylor, 2013)

2.2. Carbon pools

Carbon sinks accumulate or release sequestered carbon stored in pools namely; the above-ground biomass (AGB), belowground biomass (BGB), soil organic matter (SOM), dead wood and dead litter (Watson, 2009). The AGB refers to the living part of the tree/vegetation that is not buried in the earth, BGB refers to the parts of the vegetation that is buried in the soils, SOM however is the soil matter. Commonly considered carbon pools for carbon financing include Carbon in the AGB is the above-ground carbon (AGC), that of the BGB belowground carbon (BGC) and the carbon in SOM is the soil organic carbon (SOC) (UNFCCC, 2015). Harvested wood products are currently accepted as a carbon pool due to its long term storage of carbon (Liu & Han, 2009). Long term storage of significant amounts of carbon could serve as a basis to determine carbon pools. Carbon stock assessment is vital for transparency in carbon financing, thus determining pools helps to eliminate multiple counting and also identify and assess the uncertainties in estimated carbon values (Assefa, Mengistu, Getu & Zewdie, 2013). Knowledge on carbon pools are pertinent to estimating the amount of carbon in a terrestrial sink as this provides for monitoring the changes in terrestrial carbon sinks for mitigation and adaptation to global warming and climate changes.

2.3. Management of rubber plantations

Hevea Brasiliensis is a fast growing perennial tree which can attain a diameter at breast height (DBH) of 35 cm and a height of about 40 m, and grows well in tropical areas in tropical climates (Charoenjit, Zuddas, Allemand, Pattanakiat & Pachana, 2015). Due to its fast-growing nature it is associated with high levels of biomass, increased latex production and poses a great prospect in sequestering carbon over its lifetime (Nguyen, 2013). The rubber tree comprises the bark, cambium and then the hardwood (Schroth, Coutinho, Moraes & Albernaz, 2003).

Planting season of the trees is May/June and monitoring of the tree girth begins in November of the same year until they mature. There are prescribed measures of planting enspacement - 3m for the rows and 6m for the columns - that are strictly adhered to by management (Charoenjit et al., 2015). Tapping practice with this company is such that the trees are planted and allowed to grow until 50% attain a minimum girth of 50cm in circumference i.e. DBH of 15.92 cm where tapping begins. The age at which the desirable 50cm girth is attained is between 5 and 6 years beyond this point the latex can be harvested for all the trees (Venkatachalam et al., 2013). In some instances, some trees attain the tapping age and may have 50cm or more in girth yet they are unable to produce latex for tapping (G. Mensah, personal communication, November 14, 2016).

Depending on the clone type, various stimulation regimes are applied to influence the flow of latex. The stimulant that is applied in this context is known as ethephon which is a conventionally acknowledged stimulant according to (Chrestin, 1985) as cited in (Schroth, Moraes & Da Mota, 2004). Harvesting of latex is done every 4 days after tapping, then the tapper returns to the tree to make another 1.4mm incision for the flow of latex to continue.

The different clones of rubber found in the study area are with various levels of susceptibility to diseases (C. Kotochi, personal communication, November 16, 2016). When a plant is diseased, a trench is dug around the tree and that particular tree will be removed by the root. All neighbouring trees will be treated and monitored for signs and symptoms of the disease. The GT1 Clone is used as the standard clone for monitoring and studying all the other clones since it is more resistant to diseases.

2.3.1. Latex from rubber plantations

Latex production continues to be the utmost priority of the establishment of rubber plantations as it is used for tyres, mattress, gloves (Nguyen, 2013). The latex is made up of highly unsaturated carbon / hydrocarbons (isoprene - C_5H_8) which can yield 100 to 200 ml within 3 hours, due to its chemical makeup, biodegradation really takes a longer time (Rose & Steinbuchel, 2005).

Field latex is whitish and has the look of milk which contains a rubber fraction of 30% (Werathirachot, Danwanichakul, Kongkaew & Loykulnant, 2008). The Dry Rubber Content (DRC) fraction in some other studies is estimated to be 30 – 40 % (Petsri et al., 2013). To maximise latex flow, there should be enough direct sunshine for rubber tree, areas with high humidity and low temperatures provide a boost for increased flow of latex (Yi et al., 2014). Without these environmental factors the profitability of the rubber plantation in respect of latex cannot be realised.

2.3.2. Dry rubber content of latex

For analyses of the constituents of the latex produced by the rubber tree, the Dry Rubber Content (DRC) or the Total Solid Content (TSC) is a major factor in the market of rubber latex as it is a major determinant of the market value of the latex (Jayanthy & Sankaranarayanan, 2005; Werathirachot et al., 2008). The solid content of the rubber can be determined from the fluid latex which can be coagulated in the laboratory or allowed to naturally coagulate in the field (Khalid, 1991). The DRC or TSC of rubber is basically polyisoprene C_5H_8 (high levels of hydrocarbons) and hence a default factor (DF) of 0.88 t C t^{-1} of dry rubber can be applied to determine the carbon content (Petsri et al., 2013).This application of DF is similar to the application of conversion factor (CF) to tree biomass to determine the carbon stock of a tree (Ratnasingam, Thiruselvam & Ioras, 2016).

To compute the DRC, there is the need to first determine the DRC fraction of harvested latex (Werathirachot et al., 2008). With the Ghana Rubber Estate Limited (GREL), DRC is obtained by selecting 3 coagulated latexes per truck load and weighed (W_1). These are then passed through a creping process to form a blanket and then the blanket is weighed (C_1) (C. Kotochi, Personal Communication, November 16, 2016). A sample is cut from the blanket and weighed (W_2) for oven drying for 12 hours and then the sample is weighed (C_2) after drying. This is simplified as $[(W_1 * W_2 / C_1 * C_2) * 100\%]$ and an application of this DRC fraction to latex production values results in the DRC. The drying, weighing, drying and re-weighing to determine DRC fraction is a standard practice (Khalid, 1991; Rejikumar & Philip, 2010)

2.4. Methods of carbon estimation

Traditional methods of harvesting, drying and weighing of trees for biomass and conversion to carbon against non destructive measures such as volume data and DBH data conversion to biomass and carbon have been explored (Qureshi, Pariva, Badola & Hussain, 2012). Although the traditional tree harvesting is more accurate measure, the destructive effect does not encourage its practice relative to the non destructive methods.

2.4.1. Traditional

The tree felling process is the traditional process of obtaining carbon content of trees. The destructive approach was used to study the carbon sequestration potential of rubber plantations in Paranapoema in Brazil for 4 and 15 year old trees (Maggiotto et al., 2014). The focus of the study was the biomass accumulation rate, isotopic and soil organic carbon. Fresh weight of felled trees was obtained for all the components of AGB and BGB, subsequently the weight of biomass was computed after the components had been oven dried at a constant rate of 60°C and the water content was also determined. Carbon was subsequently measured using the Walkley-Black method. Soil samples were also taken from the plantations 20-40cm and 40-60 cm from four locations and the results indicated soil organic carbon improvement from 63.4 Mg C ha^{-1} to 66.8 and 79.3 Mg C ha^{-1} for 4 and 15-year-old plantations. This is time wasting, requires a lot of human labour to accomplish, it is not feasible for vast areas and more importantly it removes the tree from the system.

Allometric equations or biomass regression equations are models that are developed to establish a statistical relationship between tree measured attributes to estimate a non-measureable parameter such as biomass (Watson, 2009). These models are developed based on the destructive methods which help to input parameters such as DBH and height to obtain biomass and carbon as outputs. Nordh & Verwijst (2004), indicated that destructive measures perform better in terms of biomass and carbon estimations. Wauters et al., have used the destructive method to develop allometric equations for rubber plantations in the tropical rain forest region of Ghana. However, this method has been criticised not only for time consumption, but expensive, and destructive irrespective of the accuracy in measurements (Hunt, 2009). The destructive method if encouraged could equally contribute to loss of green vegetation or green cover.

2.4.2. Non-Destructive methods

The non-destructive methods of biomass estimation involve measurements of inventory data such as age, height, canopy area and wood density from the field which can be used to estimate AGB and subsequently AGC using allometric equations (Winter & Brambach, 2011; UNFCCC, 2015). Site specific allometric equations for rubber plantations in Western Ghana and Mato Grosso (Brazil) have been developed based on the destructive method (Wauters et al., 2008).

Alternatively, a comparative study of the potential of tree crop carbon sequestration was conducted for four plantation tree crops in Ghana (Kongsager et al., 2013). The non-destructive method was used to estimate AGC for rubber, cocoa, oil palm and orange trees which involved field data of age, DBH, height as inputs for allometric equations. Rubber trees turned out to have more carbon sequestered than all the plantation trees with 12-year-old rubber sequestering 61.5 t C ha^{-1} and 44-year-old at 213.6 t C ha^{-1} respectively.

In addition, carbon stock of rubber and acacia plantations have been investigated using biomass expansion factor. Volume over bark data was converted into biomass and subsequently the carbon stock was estimated (Ratnasingam et al., 2016). This method was only applied in estimating carbon in AGB and carbon (C) was calculated using a DF of 0.47, hence the equation given as C = AGB*CF. An input of more tree parameters such as height improves biomass estimation, many allometric equations for rubber using DBH for biomass estimation as eight (8) equations exist for AGB and two (2) for BGB (Yuen, Fung & Ziegler, 2016). An example is $AGB = \exp(-2.289 + 2.649 \ln(DBH) - 0.021 (DBH)^2)$ which utilizes only DBH was used by Kongsager et al. (2013) for carbon estimation for tropical tree crops including rubber plantations in Ghana.

2.4.3. Remote sensing

A combination of Geographic Information Systems (GIS) and Remote Sensing has proved useful as part of the non-destructive measures for biomass and carbon estimations as field data and satellite images are combined (Hunt, 2009). The use of remote sensing is a rather indirect approach for area biomass estimation, but there could be challenges in obtaining good data as environmental factors could impact the information retrieval from data(Brown, 2002; Lu, 2006). The practice of using remotely sensed data is to establish relationships statistically between data extracted from the satellite data and field measurements for biomass and carbon estimations (Gibbs, Brown, Niles & Foley, 2007). An integration of in situ and remotely sensed data affords a formidable alternative to the destructive process since this combination has a wider spatial coverage over a relatively shorter time and saves cost (Aalde et al., 2006). In effect remote sensing is an effective tool in biomass and forest carbon accounting especially for studies regarding changes over time (FAO, 2010). Both passive and active remote sensing have been for biomass studies which included LiDAR and Geo-Eye remotely sensed data (Bautista, 2012).

Most studies conducted on rubber plantations successfully made use of techniques of GIS and remote sensing to map the spatial distribution of rubber plantations (Tan et al., 2006; Li & Fox, 2011; Charoenjit et al., 2015). Very High Resolution Imagery from Thiachote Satellite with spectral and high spatial details has been used to estimate carbon for rubber plantations in Thailand (Charoenjit et al., 2015). The results of this study turned out that object based carbon estimation is preferred to the use of pixel based classification as image objects appearance are similar to real world objects.

2.5. Object based image analysis

Optical imagery with Very High Resolution (VHR) of less than 5 m provide fine details which help to extract tree parameters such as the crown projection area (CPA) which forms a basis for extracting tree parameters for biomass estimation (Karna et al., 2015). Image segmentation method or object-based image analysis (OBIA) can be used to extract such information from VHR, it aids in segregating image objects into distinct non overlapping elements by considering spectral, shape, textural, pattern including the location (Bakx et al., 2013). This combination of VHR imagery and segmentation based on objects proves useful for biomass and carbon estimation since it gives details for individual tree (Hay, Castilla, Wulder & Ruiz, 2005).

2.5.1. Crown projection area

Projection of tree crowns vertically over an area on the ground is referred to as Crown Projection Area (CPA) (Gschwantner et al., 2009). Tree crowns have irregular shapes, therefore measuring them could prove somewhat difficult. The measure of tree crowns is facilitated by a vertical projection of the perimeter to the ground for an averaged diameter measurement of 2 perpendicular directions (Husch, Beers & Kershaw, 2003). The CPA has been investigated to have a relationship with DBH (Karna et al., 2015; Shimano, 1997) hence with the appropriate derivation of CPA, DBH can be predicted and this is useful in carbon estimations. This relationship needs to be strong especially in instances where DBH will be modelled using CPA (Song, Dickinson, Su, Zhang & Yaussey, 2010). Figure 3 shows an example of Canopy Projection Area (CPA).

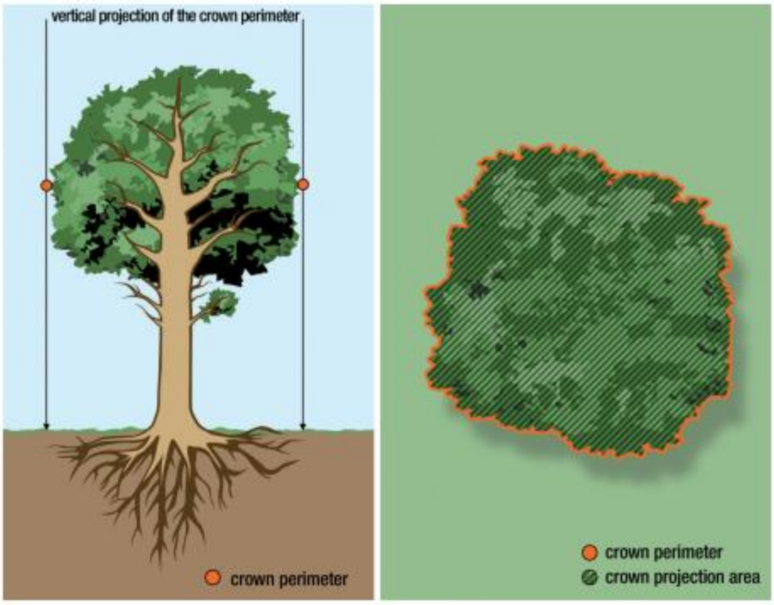

Figure 3: Crown Projection Area

Source: (Gschwantner et al., 2009)

2.5.2. Estimation of scale parameter

Scale parameter is a means to control the heterogeneity in the image segmentation process and allows for segmentation to obtain a more homogeneous image object segments (Tesema, 2015). Estimation of Scale Parameter Tool (ESP) is built on the concept of using local variances (LV) and at various scales to in a buttom up approach to generate desirable image objects that mimic reality (models) with respect to size, shape and colour (Drăguţ, Tiede & Levick, 2010). To arrive at optimum scale parameters, the thresholds in rates of change of LV (ROC-LV) indicate the scale levels at which the image can be segmented at the most appropriate level relative to scene properties in the image. The appropriate scale level helps to obtain a more homogeneous segments, thus, as the scale parameter increases, more heterogeneity is introduced (Drăguţ, Csillik, Eisank & Tiede, 2014)

2.5.3. Multi-resolution segmentation algorithm

Multiresolution algorithm combines smaller similar image objects to obtain bigger homogeneous image objects and is also considered as a region based algorithm (Gao, Siu & Hou, 2001). This region based algorithm works on the principle of reducing average heterogeneity of image objects per given resolution thereby promoting higher homogeneity in the image objects. Four main steps characterize the procedure for multi-resolution segmentation including; segments start from single to merge other pixels in series of loops until objects are homogeneous, initial starting pixels find best fitting neighbours for merging, best image object replaces a non-mutual best fitting pixel to turn into a nouvelle image object and finds best fitting partner, and finally, when the best fitting is mutual, a merger of image objects are observed (Rejaur Rahman & Saha, 2008; Trimble, 2014)

2.5.4. Watershed transformation

Watershed transformation algorithm is conducted to identify individual trees from a cluster, therefore the points where the clustered or intermingled crowns seem to touch each other serve as joining blocks. These points of joints were identified as valleys (watersheds) and were used as the basis for splitting to eliminate overlapping crowns (Derivaux, Forestier, Wemmert & Lefèvre, 2010). By adopting this method, tree crowns that touching each other are separated into individual crowns.

2.5.5. Morphology

Morphology algorithm is used to refine image objects segments based on mathematical morphology to smoothen and reshape the boundaries of objects (Shafri, Hamdan & Saripan, 2011). It incorporates the shape and size of the object to smoothen the boarders of the image in order to give shape to the image objects.

2.5.6. Accuracy assessment

A combination of topological, geometric and visual techniques are employed to assess the accuracy of the segments created using manually digitized reference polygons of the crowns of the rubber trees (Moller, Lymburner & Volk, 2007).

2.6. Google Earth imagery

The use of virtual globes for studies and navigation has become very important in contemporary times due to its three-dimensional representation of the Earth, user friendliness and flexibility in changing views and positions of any portion of the earth (Rozanda, Ismail & Permana, 2015). Some limited information relating to the image processing include balancing of colour, as well as image warping to produce large mosaics (Yang, Jiang, Luo & Zheng, 2012). Application of virtual globes for routings and studies have become an essential aspect of life in modern era owing due to its three-dimensional representation of the Earth, flexibility as well as user friendly interfaces that aid in switching between views and location of the earth (Rozanda, Ismail & Permana, 2015). The Google Earth Imagery comprises three spectral bands of red, green and blue otherwise known as RGB with less known spectral analysis applied to it yet it has proved useful in many studies (Visser, Langdon, Pauchard & Richardson, 2014). Visual interpretation as well as visual image object identification is enhanced and made relatively easier with Google Earth Imagery. In as much as automatic algorithms can detect image objects at relatively faster rates, it takes time for the human eyes to do such detection especially as it varies per person (Joseph, 2005). Yet, the human intellect helps to harmonize characteristics as location, size, texture, colour, shape and pattern relative to real world for deductive analysis in ways which is not currently possible with any machine based algorithm. Thus, with the aid of special tools such as zooming in and different angles of look among others embedded in the google map software, computer aided object based analysis have become relatively less difficult and can be done more frequently to the convenience of the researcher (Rozanda et al., 2015). Other tools that are available include viewing images across time, drawing up polygons and marking up locations based on points. These can subsequently be exported into a Geographic information Systems environment for further analysis or integration with other data. However, remote information given by Google Imagery requires verification from the field to ascertain the extent to which deductions made from Google Earth Imagery are as real as what actually exists per location.

Several scientific studies have been conducted using Google Earth Imagery. Rozanda et al., (2015) conducted a comparative study of two different methods of segmentation K-Means Clustering and Normalized RGB Colour Space on Google Earth Imagery. The results of the study indicated that although K-Means clustering could show about 40.5% pixels and Normalized RGB colour Space could show about 47.01% pixels as vegetated areas, K-means proved to have a higher accuracy in image clustering relative normalized RGB space method. Subsequently, this author recommends the use of Google Earth Imagery for further research in as much as segmentation analysis is concerned. A further use of Google Earth imagery for extracting vegetation has been conducted using a robust Back Propagation Neural Networks (BPNN) in Hue, Saturation and Value (HSV) Space (Almeer, 2012). Ploton et al. (2012), used Google Earth imagery in comparison with IKONOS imagery for the scientific study of assessing aboveground tropical forest biomass in spite of its spectral limitations. The author employed textural analysis using the Fourier Textural Ordination (FOTO) of canopy images on Google Earth and IKONOS images for aboveground biomass estimation.

2.7. Statistical tests

The branch of science associated with studies based on data collection, organization, summarizing and analysing the data to draw meaningful conclusions constitutes statistics (Bluman, 2012). It may include descriptive statistics of describing data available for a study or drawing samples from a population to make inferences about that population.

2.7.1. Parametric and non-parametric tests

To test hypothesis the decision is based on the data type as data normality is important since it determines the type of tests to subject the data to (Razali & Wah, 2011). If the data happen to be normally distributed, then a parametric test could be selected to test the hypothesis, on the contrary, a data that does not assume normality can be subjected to non-parametric testing (Bluman, 2012). Examples of normality tests include the Shapiro Wilk (SW) and Kolmogorov Smirnov (KS) tests with the first considered suitable for less than 50 samples and KS tests considered as a belonging to a super class (Razali & Wah, 2011). Normal distribution of data requires parametric tests such as Analysis of Variance (ANOVA) tests and t-tests, whilst non-parametric tests include Kruskal-Wallis, Mann Whitney-U tests, Wilcoxon tests among many others (du Prel, Röhrig, Hommel & Blettner, 2010). Normality tests of data is important since it helps to give valid results to all subsequent statistical tests.

2.7.2. Regression analysis

Regression analysis aid in determining the quantitative relationship that exists between two variables (dependent and independent)(Razali & Wah, 2011). Thus the extent to which one variable(independent) can be used to predict the other variable(dependent) can be so established (Bluman, 2012). Regression analysis is commonly used for biomass estimation studies (Tsendbazar, 2011) as they are used to develop models relate CPA to DBH. Accuracies of such predictive models can be used to produce biomass and carbon. Samples size in regression models are important since they affect the authenticity and accuracy of such models, hence as a rule of thumb, events per variable in any regression model should not be less than 10 (Concato, Peduzzi, Holford & Feinstein, 1995; Peduzzi, Concato, Feinstein & Holford, 1995).

3. MATERIALS AND METHODS

3.1. Study area

3.1.1. Geographic Location

The study area as depicted in Figure 4 is located at Abura around Agona the District capital of the Ahanta West District of Ghana. It is located between latitudes 4º 53´N - 4º 48´N and longitudes 2º 7´ 30" W and 2º 47´W closer to the equator (Kottek et. al., 2006). The Ahanta West district is encompassing an area of 59,100 ha with 70.5% of the area being rural and a total population of 106, 215 comprising 50,999 males and 555,216 females (Ghana Statistical Service, 2012). Study area was delineated to cover a range of different ages, accessibility during data collection and cloud free Google earth image data.

3.1.2. Topography and Vegetation

The terrain is relatively flat with few slopes as the highlands are in the range of about 100m - 152.4m according to the Western Regional Coordinating Council as cited in (Danso-Manu, Poku & Fayorsey, 2013). Acrisol and ferralsol soil types are usually found around the few highland areas (Driessen, Deckers & Spaargaren, 2001). The well drained acidic soil in the area has 76% sand, 22% clay and gravels at 10 - 60 cm deep which has been a major support in rubber plantation establishment in the area (Wauters et al., 2008).

The study area falls in a section of the Ghana Rubber Estate Limited's Division 1 rubber plantation field. The total surface area spans 1,492.39 ha of mature rubber plants under tapping and they have varying ages due to different years of planting. The current spatial extent (4º 53´N - 4º 48´N and 2º 7´ 30" W and 2º 47´W) of the rubber plantation cannot expand since the total land concession available to the company has been fully utilized.

3.1.3. Climate

The Ahanta West district is situated in the tropical rainforest region in the south-western parts of Ghana with south-western equatorial climate. And like all equatorial regions the major seasons are two which include the rainy and dry seasons summarized in Table 1.

Table 1: Seasonal periods in South-western Ghana

Condition	Month	Recordings
Rainfall	April – July and December–March	0-500mm per month 1200-1800 per annum
Dry	October–November and August–September	24º C and 27º C per annum (average)
Temperature	January to December	15º C and 40º C (extreme)

Source: (Wauters et al., 2008)

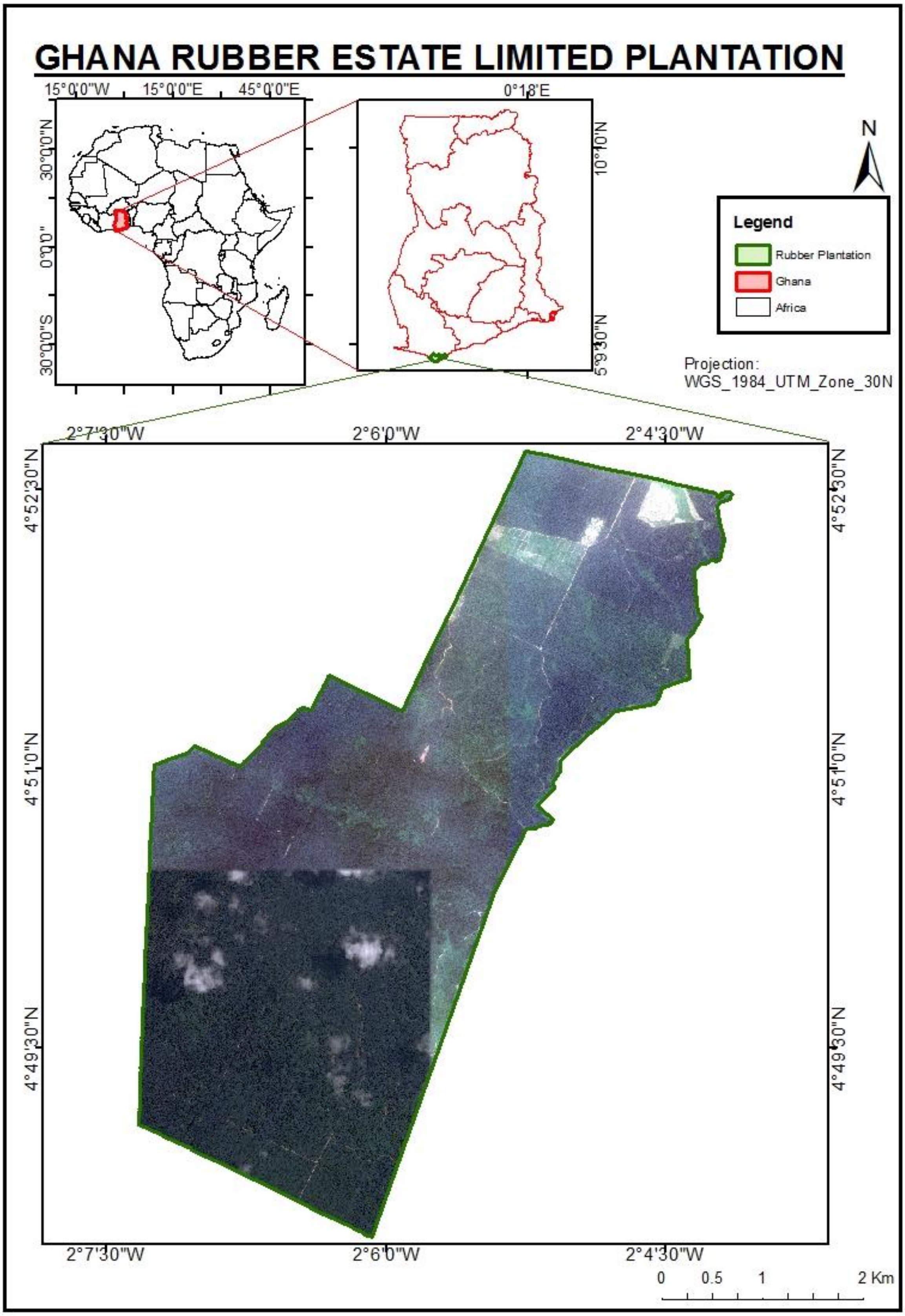

Figure 4: Study Area

3.2. Materials

Details of field instruments used are specified in Tables 2 and 3 specifies various software packages for different analysis to yield the desired outcome.

Table 2: Field Instruments and their uses

No.	Instrument	Use
1	GPS	Sample point coordinates/ Navigation
2	IPAC	Location of sampling plot
3	Printed Map of Study Area	Geospatial Navigation
4	Surveyor's Meter Tape	Measuring distances
5	Diameter tape	DBH measurement
6	Chalk	Tree Markings
7	Clip board	Hold data sheets
8	Computer	Data analysis, Processing and Reporting.
9	170 cm stick	DBH_{170} measurements

Table 3: Software packages and their uses

No	Software Package	Use
1	Ecognition	Image Segmentation
2	ArcGIS	GIS analysis / Mapping
3	Erdas Imagine	Image processing
4	Microsoft Word	Writing thesis
5	Microsoft Powerpoint	Presentation
6	Microsoft Excel	Statistical analysis
7	SPSS	Statistical analysis
8	Mendeley	Referencing
9	Foxit Reader	PDF preparation
10	SAS Planet.exe	Google Earth Imagery Acquisition
11	ESP Tool	Scale parameter Estimation

3.3. Methods

The methods used entirely to complete the study is shown in Figure 5 as a flowchart. For the scope of this work, the site specific allometric equations for the Hevea brasiliensis specie was preferred over other ones. Site specific equations classified as TIER 3 are associated with higher levels of accuracy, hence the choice of a site specific equation for this study (Goetz et al., 2009). Tree girth measured at a height of 170 cm (C_{170}) are for rubber biomass and carbon estimation due to the bark removal, (Wauters et al., 2008; Charoenjit et al., 2015). The estimations are based on a stated relationship for the foliage, stem and roots which permit for direct estimation of aboveground carbon and belowground carbon using field C_{170}. The results of the allometric equation gives carbon values directly, hence no need for conversion factor since the study focuses on carbon (Wauters et al., 2008).

To achieve the set objectives three levels of data processing were employed.

1. For objective 1, latex production was rescaled from production per acre to production per plot level for latex carbon estimation at plot level. The carbon composition at plot level per age class was subsequently compared.
2. For objective 2, both aboveground and belowground carbon was calculated using allometric equations for plot level per age class. The allometric equations developed for rubber plantations in Western Region of Ghana permits for the use of C_{170} to compute both AGC and BGC (Wauters et al., 2008). Latex carbon used for the comparison was drawn from objective 1.
3. Finally, with the aid of Google Earth Imagery, OBIA was conducted for the purposes of carbon modelling.

3.3.1. Data

Datasets used to achieve the first objective of differences in latex carbon content for different ages include; sample point coordinates, age, Dry Rubber Content (DRC) fraction values, latex production data and tree density per plot.

To achieve objective two of comparing the differences in carbon between aboveground, below ground and latex carbon the following data were used; age, tree density per plot, and field DBH measurements were used for aboveground and belowground carbon. Latex carbon values obtained for objected one were adapted and used to aid the comparative differences between the three pools.

The datasets needed to achieve the final objective of using Google Earth derived CPA to predict DBH required the use of VHR Google Earth Imagery, field measured CPA and field measured DBH. Other data which were received from GREL are summarised in Table 4.

Table 4: Data support from GREL

Type of Data Made Available from Company	APPENDICES
Block ID, Blocks, Size, Year of Planting, Latex production per annum, Total Latex produced per stand.	Appendix 1
Dry Rubber Content Fraction	Appendix 2

3.3.2. Google Earth image data

The Google Earth data used for this research was obtained using the SAS Planet software. A shape file of the study area with the WGS 84 coordinate system was loaded into the software to identify the area of interest. The zoom function was used to ensure that all image objects appear very clear throughout the area of interest after which download was initiated. The download was set to the highest permissible zoom level of 22 at which very high resolution images can be obtained. The downloaded image came fully georeferenced and was in the UTM WGS 84 Zone 30N coordinate system and in the .ecw format. The parameters of the Google Earth Image can be found in Appendix 3.

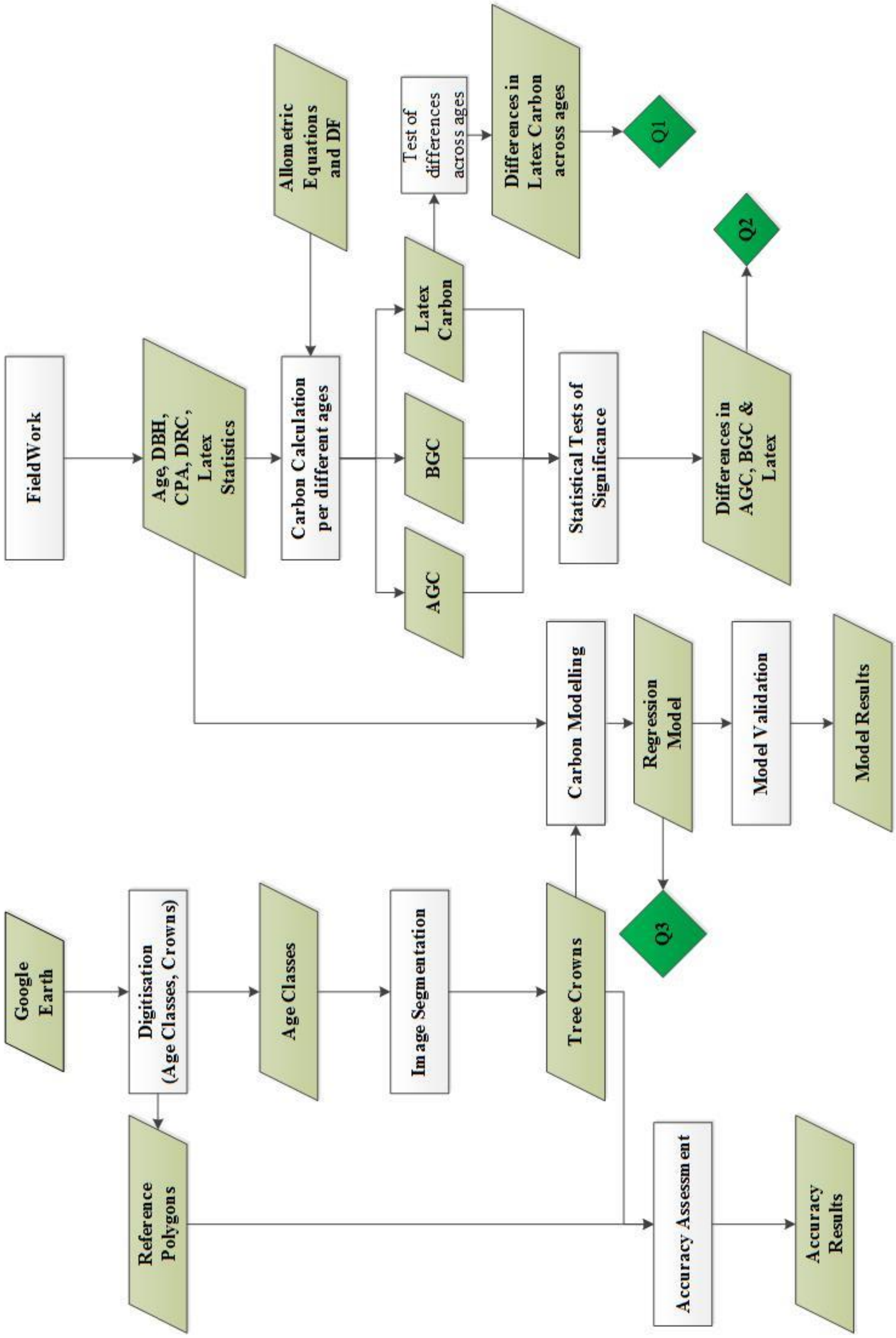

Figure 5: Methods workflow

3.4. Data collection

3.4.1. Sampling design

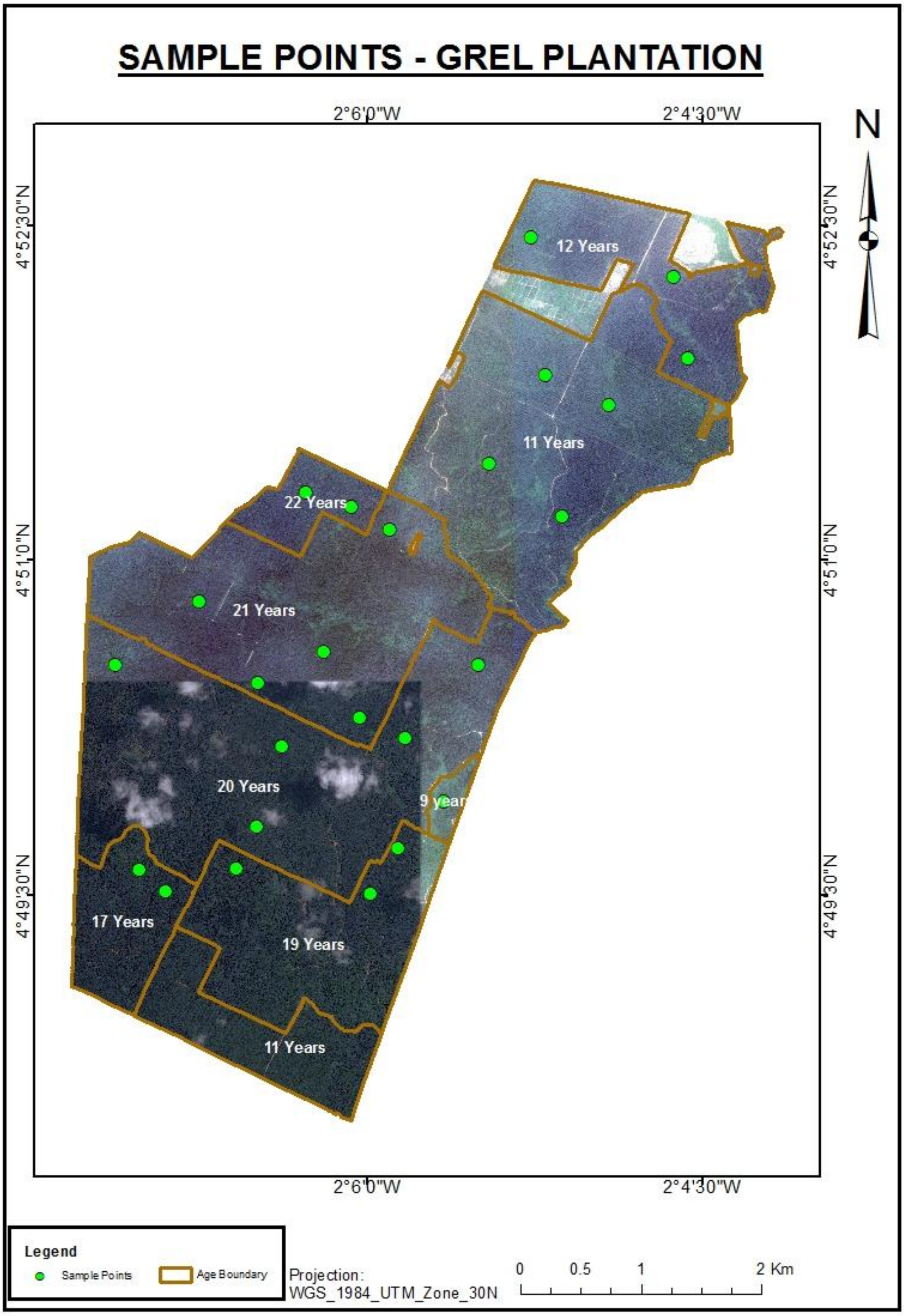

Figure 6: Sample Points Distribution in the various age classes

Due to the homogeneous structure of the plantation and the differences in age, the stratified random sampling design was adopted for the study (Omair, 2014). Stratification of rubber plantations with respect age for biomass studies has been adopted to since the differences in tree parameters result from the different years of planting (Wauters et al., 2008; Charoenjit et al., 2015). With the aid of age data from GREL, the study area was stratified based on the age categorization of the plantation. Eight different strata with respect to ages were identified from data made available by GREL as 22, 21, 20, 19, 17, 12, 11 and 9 with varying tree densities per plot (Appendix 4).

The plantation is divided into separate planting blocks by the company thus, there was a total of 100 planting blocks within the study area. A total of 25 sample points of 500 m² circular plots (UNFCCC, 2015) were laid in the 25 blocks out of the 100 divisional blocks in the plantation. These sample plots were generated in the excel environment with the aid of random numbers to avoid bias.

Data collection sheets (Appendix 5) were developed using Microsoft Excel software and loaded into an IPAQ and hard print versions were produced as back up for site information collection. Maps with the sample points (Figure 6) were printed as backup to the GARMIN GPS which had the sample point coordinates loaded onto for navigation purposes. In the field, the GPS and paper maps aided in locating the sample points. Upon navigation to these points circular plots (Figure 7) of radius of 12.62m were laid with the aid of the surveyor's tape. Within each plot and across the different age categories, the DBH and CPA of individual trees were measured alongside the planting density. All trees within the plots were marked with a field chalk and had their DBH measured since none had a DBH of less than 10cm. To ensure consistency, a 170cm stick was used to aid in identifying the diameter at breast height of 170cm (DBH_{170}) and the measurements recorded on the field data sheets and on the IPAC. The tree crowns were equally measured to aid in the image segmentation. For the field data, GREL also made available a complete stock of the tree densities for all of its blocks for the whole study area. Production data is also comprehensively recorded, thus latex production per tree was readily available for all the productive blocks.

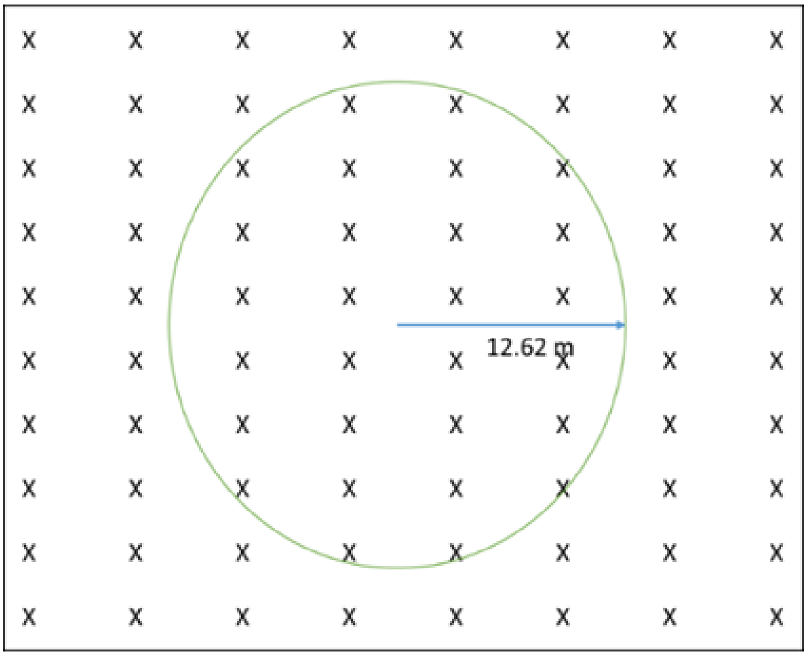

Figure 7: 500m² Sample Plot Size

3.5. Objective 1: To determine the differences in carbon from latex for the different ages categories.

To ensure standardization of carbon from latex in tandem with field measured diameter at breast height (DBH) latex production was computed for all plots at the level of $500m^2$ (0.05ha) from the latex production data (Appendix 1) for the different ages. This was important to make comparison among the carbon pools possible since they will be at the same scale. This was done by dividing the plot area 0.05ha by the total area that each plot was located and multiplied by the total production for that particular area. This is summarised below in Equation 1. This was necessary since all other carbon values to be computed were at the plot level of 500 m^2.

Latex per plot = (0.05ha/Area ha) * Latex (kg) *Equation 1: Latex production (kg) per 500 m^2*

DRC= Latex produced (kg) * DRC% *Equation 2: Dry Rubber Content (kg per 500 m^2)*

Latex Carbon = DRC * 0.88 t C t^{-1} *Equation 3: Latex Carbon Content (t C per 500 m^2)*

After obtaining the latex produced per plot for all the plots within all the ages, average DRC fraction (60.4%) (Appendix 2) of the latex was applied using Equation 2 based on company data. This resulted in actual DRC per plot (kg per $500m^2$) and was converted to carbon using the default factor of 0.88 t C t^{-1} (Equation 3) to obtain the carbon values per plot in tons of carbon per 500 m^2 (t C per $500m^2$) (Petsri et al., 2013). The carbon was rescaled from t C per 500 m^2 to tons of carbon per hectare (t C ha^{-1}) (Appendix 6), to enable comparisons with other carbon pools.

A statistical test of normality was conducted using the Shapiro-Wilk's test of normality prior to a parametric statistical test (One-way ANOVA). A pairwise multi-comparison factoring in the Bonferroni effect correction was conducted. This correction is a conventional way to reduce the higher probability of committing a type I error if many tests are performed by dividing the alpha (α) by the number of tests performed (M) (Greenacre & Primicerio, 2013).

3.6. Objective 2: To compare the differences in the contribution of latex, aboveground and belowground carbon pools to carbon sequestration.

The DBH_{170} per age class was converted to circumference measured at a height of 170 cm (C_{170}) using Equation 4 for all the plots. This was necessary to fit into the allometric equation to be used for the carbon estimation.

$C_{170} = \pi * DBH_{170}$ *Equation 4: DBH to girth conversion (cm)*

To compute the AGC, Equation 5 (foliage carbon) and Equation 6 (stem carbon) were computed separately and back transformed using Equation 7 (Wauters et al., 2008). A summation of the foliage carbon and stem carbon resulted in aboveground carbon (kg) per $500m^2$. The aboveground carbon (kg C per $500m^2$) per plot per the different ages were rescaled to tons of carbon per hectare (t C ha^{-1}) (Appendix 7).

$\ln Y = -6.118 + 1.857 * \ln C_{170}$ *Equation 5: Foliage carbon allometric equation (kg C)*

$\ln Y = -7.260 + 2.904 * \ln C_{170}$ *Equation 6: Stem carbon allometric equation (kg C)*

$EXP^{(\ln Y)}$ *Equation 7: Back transformation formula*

To compute belowground carbon, the converted field DBH_{170} to C_{170} were imputed in to allometric equation for belowground carbon for rubber trees. Additionally, belowground carbon was calculated at the plot level (kg C per $500m^2$) using Equation 8, Equation 7 was further used to back transform and obtain the desired carbon values for belowground carbon (Wauters et al., 2008). The below ground carbon (kg C per 500m²) per plot per the different ages were rescaled to tons of carbon per hectare (t C ha^{-1}) (Appendix 7).

$$\ln Y = -4.996 + 1.872 * \ln C_{170}$$ *Equation 8: Belowground carbon allometric equation (kg C)*

Shapiro Wilk's test of normality was conducted on the carbon values for the various pools (latex carbon, aboveground carbon and belowground carbon). The Kruskal Wallis non parametric test was performed to test the null hypothesis that there exists no differences in the carbon pools (aboveground, belowground and latex carbon).

A post-hoc effect size test (Kruskal Wallis test) and controlling for Bonferroni effect were performed to identify which pair of rubber carbon pools (AGC, BGC and Latex) had significantly different carbon values.

3.7. Objective 3: To analyze the relationship between Google Earth derived canopy projected area and diameter at breast height

3.7.1. Image segmentation process

The estimation of scale parameter (ESP) tool was loaded into the eCognition software together with the Image for the estimation of suitable scale for the segmentation process. Figure 8 below shows the threshold at which the Google Earth Imagery could be objectively segmented. The first image shows the whole trend and the second image zooms in to further see the value where the ROC line peaks. A scale factor of 20 was chosen for the segmentation.

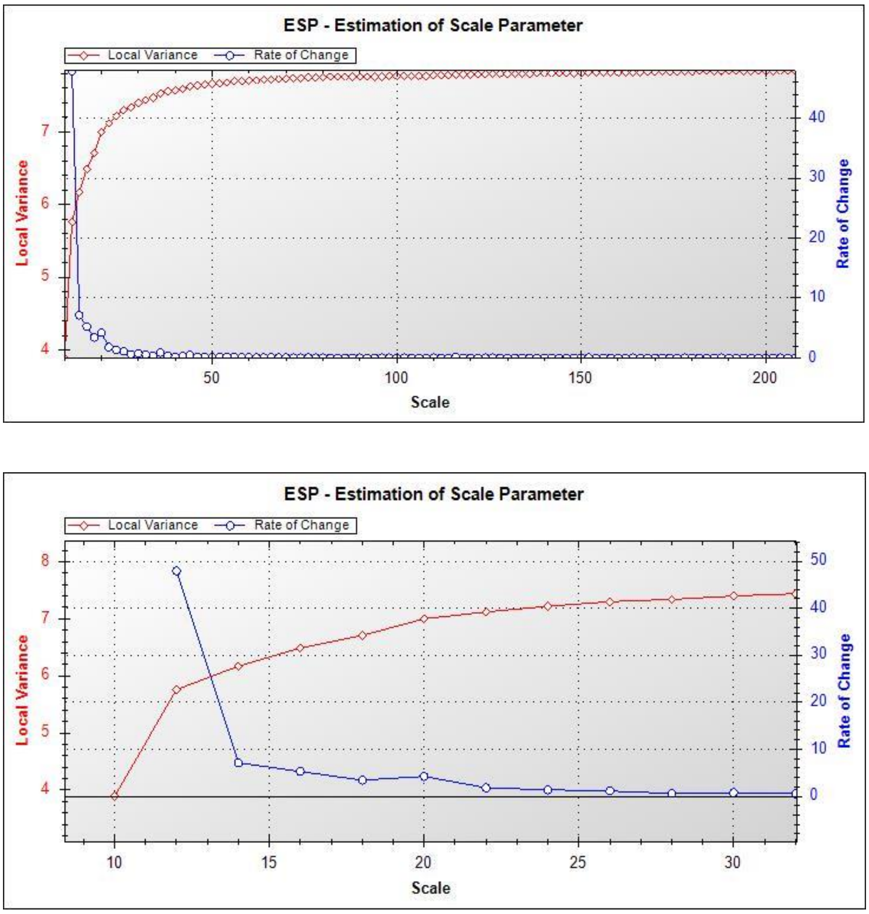

Figure 8: ROC-LV for ESP

The Google Earth image was digitised into the different age classes of 22, 21, 20, 19, 17, 12, 11, and 9-year-old stands. The digitised classes were used to extract each age class from the Google Earth image for the segmentation process to be conducted on age by age basis. Manual delineation of the crowns of the individual trees observed in the plots and identified on the Google Earth image was conducted. The manual delineation of individual crowns was also performed with the aim of conducting an accuracy assessment to validate the segmented image objects.
Although there exists other segmentation algorithms, the multi-resolution segmentation algorithm is widely used to successfully obtain image object segments (Hay et al., 2005; Rejaur Rahman & Saha, 2008). The scale parameter used for the multi-resolution segmentation was 20 with shape and compactness set at 0.5 each. This resulted in the generation of image object segments, however, not all the segments were proper, therefore the need to refine the segments.

Due to the mosaicking of several images to form the Google Earth imagery, there were shadows and clouds in the imagery which were masked using the brightness values. These shadows and clouds were merged separately and classified as such and excluded from subsequent analysis.

This algorithm was used to refine the image segments to split large crowns and clustered crowns into separate tree. The factor used here was 10 pixels since maximum field observation of Tree crown was observed at 3m and the Google Earth Image has a resolution of 30cm.

The results of the watershed transformation did not come out as the desirable (rounded) segments, hence the need for the morphology algorithm to be run. The Open Image object parameter was adopted to remove pixels which were separated from the segmented objects. A circular mask was also created for defining the size and shape to bring about the almost circular shape of tree crowns.

Undesirable image objects were removed after the watershed transformation and morphological operations. Image objects which were unwanted segmentation such as tiny and elongated objects were removed on the basis of roundness, area of pixel attributes. The rule set which refers to the command processes employed in the segmentation process is as shown below in Figure 9.

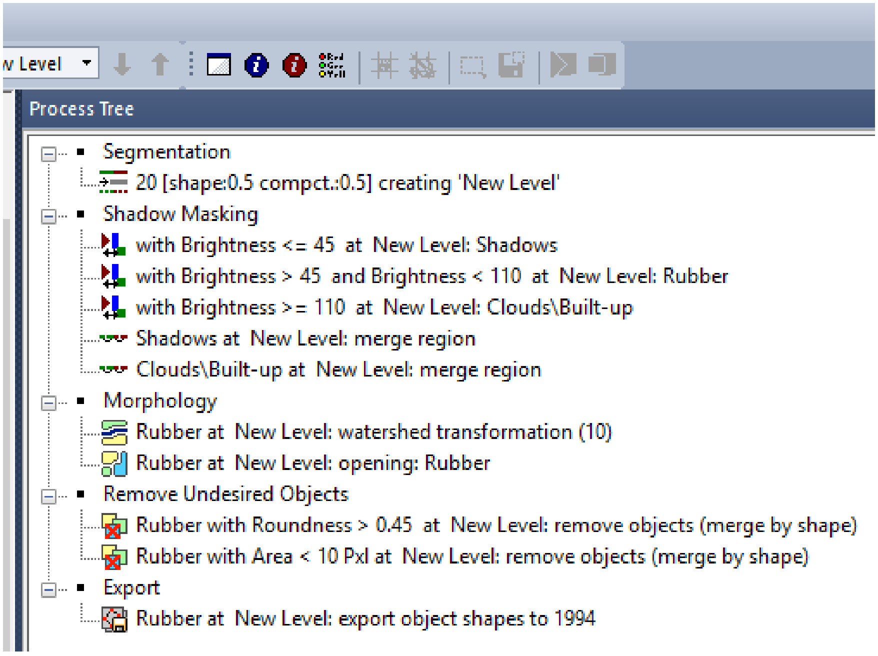

Figure 9: Segmentation rule set

3.7.2. Validation of segmentation

A combination of topological, geometric and visual techniques was employed to assess the accuracy of the segments created using manually digitized reference polygons of the crowns of the rubber trees. This was carried out by considering the extent to which reference polygons and image object segments match each other in terms of position, size and shape by at least 50%. The overall accuracy of the segmentation results was determined using the segmentation goodness of fit, the "D" in Equation 9. This was made possible by first computing over-segmentation using Equations 10 and under-segmentation using Equation 11. The Figure 10 below shows the matching conditions as expressed by (a) over 50% match (b) same shape and size of segments with reference objects but for differences in position; (c) and (d) segments and reference objects may be of match with respect to position but not of same spatial extent. Common areas of overlap are indicated in red whereas areas of differences are identifiable in blue and green respectively.

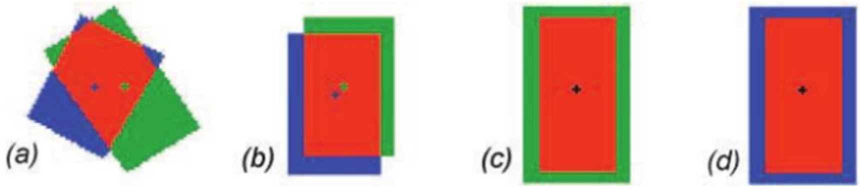

Figure 10: Matched cases of extracted objects

Source: (Zhan, Molenaar, Tempfli & Shi, 2005)

$$D_{ij} = \sqrt{\frac{Over-Segmentation_{ij}^2 + Under-Segmentation_{ij}^2}{2}}$$ *Equation 9: Segmentation Goodness*

$$Over-Segmentation_{ij} = 1 - \frac{area(x_i \cap y_j)}{Area(X_i)}, y_i \in Y_i^*$$ *Equation 10: Over-Segmentation*

$$Under-Segmentation_{ij} = 1 - \frac{area(x_i \cap y_j)}{Area(Y_i)}, y_i \in Y_i^*$$ *Equation 11: Under-Segmentation*

3.7.3. Model development

To analyse the relationship between then Google Earth derived CPA and DBH for the purposes of carbon modelling, regression analysis was conducted. A non-linear relationship between the CPA which was the dependent variable and the DBH as an independent variable was established. This was to help evaluate the extent to which the CPA could predict DBH accurately for the purposes of carbon modelling using the OBIA procedure.

Trees with one to one matching in terms of those identified on the field and those obtained from the segmentation process of the Google Earth imagery were used. From the identified 102 trees 70 trees were used for the model development and the remained 32 were used for the validation. The Root Mean Square Error (RMSE) was computed by comparing the predicted values derived from the segmentation process against the observed values from the field shown by Equation 12.

$$RMSE = \sqrt{\sum \frac{(DBH_p - DBH_o)^2}{N}}$$ *Equation 12: Root Mean Square Error*

4. RESULTS

4.1. Objective 1: To determine the differences in carbon from latex for the different ages categories.

The results of the latex produced by rubber per plot (500m^2) from which carbon was subsequently computed is shown in Table 5. The 22-year-old stand which consisted of 25 trees produced the highest latex of 1,652.98 kg equivalent to 878.59 kg of carbon per plot. The 21-year-old stand with 24 trees recorded 1,545.07 kg of latex produced equivalent to 821.24kg C per plot whilst the least latex production was recorded by the 9-year-old stand which recorded 195.46kg of latex from 25 trees also equivalent to 103.90kg C per plot. The result revealed that latex produced from stands that were 20 years and above generated about 1000kg and above whilst latex production from stands below 20 years were less than 1000kg. The stands above 20 years produced 480.54kg C – 878.59kg C whereas stands below 20 years produced 103.90kg C – 482.51kg C.

Table 5: Latex production rescaled from total planted surface to production at plot level (kg per 500 m^2)

Age of Rubber Stand	Number of plots	Number of trees per plot (500m^2)	Latex produced (kg) per plot (500m^2)	Latex Carbon (kg C) per plot (500m^2)
22	1	25	1652.98	878.59
	2	24	1612.80	857.24
21	1	22	1245.93	662.23
	2	23	1265.80	672.80
	3	22	1294.08	687.83
	4	17	1442.81	766.88
	5	24	1545.07	821.24
20	1	21	1442.46	766.70
	2	19	1090.23	579.48
	3	23	904.09	480.54
	4	21	1249.00	663.87
	5	22	1059.84	563.33
19	1	17	742.07	394.43
	2	24	723.05	384.31
	3	19	907.79	482.51
17	1	21	801.84	426.20
	2	23	745.98	396.50
12	1	23	371.20	197.30
	2	25	476.95	253.51
	3	25	385.81	205.07
11	1	22	332.42	176.69
	2	23	329.61	175.20
	3	23	391.99	208.35
	4	21	318.68	169.39
9	1	25	195.46	103.90

Figure 11 and Table 6 represent the mean carbon (t C ha^{-1}) from latex computed for the different ages of the rubber plantation. The mean latex carbon content ranged from 2.08 t C ha^{-1} for the 9-year-old stand to

17.36 t C ha^{-1} for 22-year-old stand. The difference in carbon for ages 22 and 21 was 2.92 t C ha^{-1}, a difference of 2.22 t C ha^{-1} was observed between ages 21 and 20, further difference of 3.81 t C ha^{-1} was recorded between ages 20 and 19, for ages 19 and 17 the difference was at 0.18 t C ha^{-1}, ages 17 and 12 recorded a difference of 3.86 t C ha^{-1}, that of ages 12 and 11 was 0.72 t C ha^{-1} and the difference between ages 11 and 9 was 1.57 t C ha^{-1}.

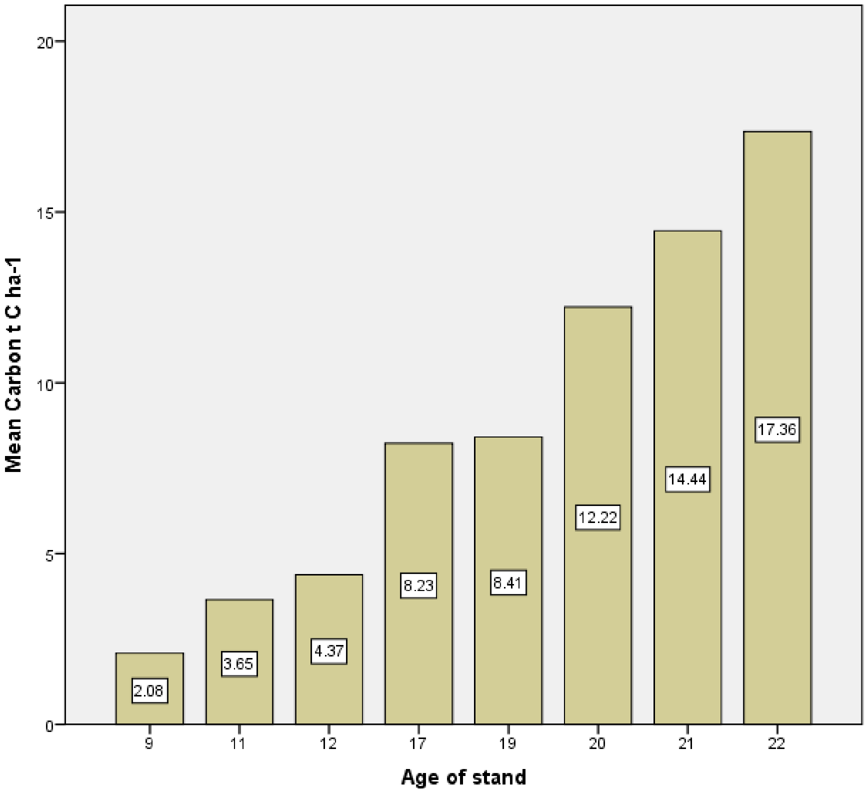

Figure 11: Differences in carbon (t C ha-1) from latex per age class

Table 6: Means of Carbon from Latex (t C ha-1) for different ages

Age	N	Mean	Std. Deviation	Std. Error	95% Confidence Interval for Mean		Minimum	Maximum
					Lower Bound	Upper Bound		
22	2	17.36	0.30	0.22	14.62	20.09	17.14	17.57
21	5	14.44	1.38	0.62	12.73	16.15	13.24	16.42
20	5	12.22	2.17	0.97	9.52	14.92	9.61	15.33
19	3	8.41	1.08	0.62	5.73	11.09	7.69	9.65
17	2	8.23	0.42	0.30	4.48	11.97	7.93	8.52
12	3	4.37	0.61	0.35	2.86	5.88	3.95	5.07
11	4	3.65	0.35	0.18	3.09	4.21	3.39	4.17
9	1	2.08	.	.	.	.	2.08	2.08

The Shapiro-Wilk's normality test revealed that the data was normally distributed: F (25) = 0.928, p= 0.79 (Appendix 8). A one-way ANOVA test to compare the means of latex carbon across the different ages indicated a statistically significant difference: F (7, 17) = 45.028, p<0.05, (Appendix 9).

A post-hoc multi-comparison test (whilst applying the Bonferroni correction) indicated that the mean latex carbon for age class 22 was significantly different from age classes 20 at p=0.007, 19, 17,12, 11 and 9 at p=0.000. For age 21, the significant difference in latex carbon was recorded in comparison to age classes 19, 17, 12, 11 and 9 at p=0.000 and the latex carbon for age group 20 was observed to be statistically different from age groups 12, 11 and 9 at p=0.000 (Appendix 10). From Table 7 where the significant differences among the different years are shown, the positive sign denotes significant differences and the negative sign shows non-significant difference between the ages. Age 22 was significantly different from ages 20, 19, 17, 12, 11 and 9. Age 20 was significantly different from 12, 11 and 9 years, beyond which no significant differences are recorded.

Table 7: Summary of Pairwise multi-comparison of latex carbon (t C ha^{-1}) with Bonferroni correction

AGE	22	21	20	19	17	12	11	9
22	-	-	+	+	+	+	+	+
21		-	-	+	+	+	+	+
20			-	-	-	+	+	+
19				-	-	-	-	-
17					-	-	-	-
12						-	-	-
11							-	-
9								-

(+) significant difference
(-) no significant difference

4.2. Objective 2: To compare the differences in the contribution of latex, aboveground and belowground carbon pools to carbon sequestration.

The field measured diameter at breast height of 170m (DBH_{170}) used for the aboveground carbon (AGC) and belowground carbon (BGC) computation is shown in Figure 12 (Appendix 11). At the plot level of 500m² the mean DBH_{170} for the youngest rubber stand of 9 years is given as 16.96cm which is 4.89% less than the highest DBH_{170} (25.78cm) for the 22-year-old rubber stand. The difference between the highest DBH_{170} and the least DBH_{170} is 8.82cm and this exists for the ages of 9 and 22 years.

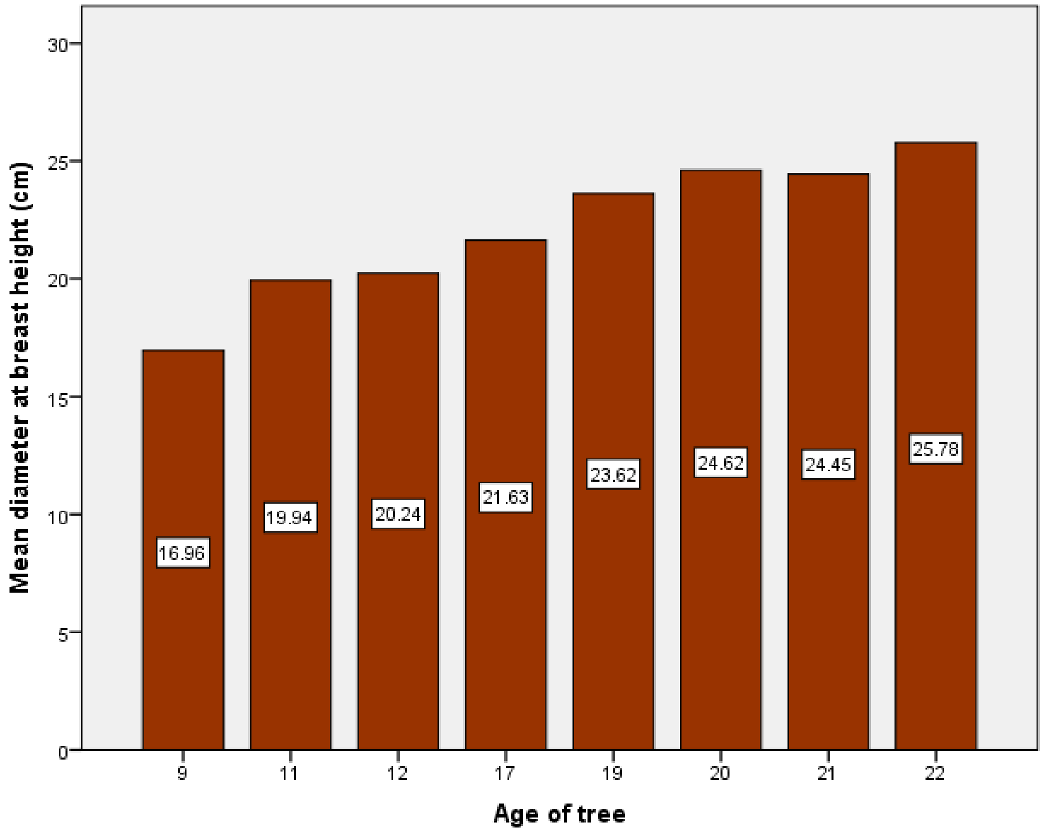

Figure 12: Mean DBH_{170}(cm) per age class for aboveground and belowground computation

From Table 8, AGC recorded higher sequestered carbon values relative to belowground carbon below (BGC) and latex carbon. At age 9, AGC recorded a higher carbon content of 38.08 t C ha^{-1} compared to 5.77 t C ha^{-1} for BGC, and 2.08 t C ha^{-1} to latex. At age 19 (10 years after), AGC recorded a higher carbon content of 87.11 t C ha^{-1} in comparison to 9.24 and 9.13 t C ha^{-1} for BGC and latex, respectively. At age 22, AGC recorded 126.6 t C ha^{-1}, BGC recorded 12.47 t C ha^{-1}, and latex recorded 17.36 t C ha^{-1}. The decreasing root to shoot ratio was observed for the ages 9, 11, 17, 19, 20, 21 and 22 were found to be 0.152, 0.129, 0.127, 0.119, 0.106, 0.106, 0.104 and 0.098 respectively for the individual years.

Table 8: Distribution of sequestered carbon in the aboveground, belowground and latex carbon pools according to age

		Carbon per ha (t C ha^{-1})			Total Carbon (t C)		
Age	**Area (ha)**	**AGC**	**BGC**	**Latex**	**AGC**	**BGC**	**Latex**
22	45.91	126.60	12.47	17.36	5,812.21	573.88	796.77
21	293.84	95.81	9.95	14.44	28,149.87	2,938.40	4,244.22
20	342.07	89.78	9.50	12.45	30,717.89	3,249.67	4,178.73
19	86.07	87.11	9.24	9.13	7,496.70	791.84	723.85
17	60.89	67.26	8.01	8.22	4,097.90	487.12	500.82
12	171.30	61.56	7.82	4.37	10,552.08	1,336.14	749.15
11	457.68	54.04	6.97	3.65	24,714.72	3,203.76	1,669.39
9	34.74	38.08	5.77	2.08	1,323.59	201.49	72.26

The total area considered in this study was 1,492.50 ha with total AGC of 112, 864.96 t C, BGC 12, 782.30 t C and Latex carbon of 12,935.19 t C. The 20-year-old rubber stand had a larger planted surface of 342.02 ha and recorded the highest AGC and BGC compared to the 21-year-old rubber stand which had 293.84 ha yet the latex carbon was higher for the 21-year-old stand. The least total carbon sequestered was by the 9-year-old plantation which had a planted surface of 34.74 ha, AGC 1,323.59 t C, BGC of 201.49 and latex carbon of 72.26 t C.

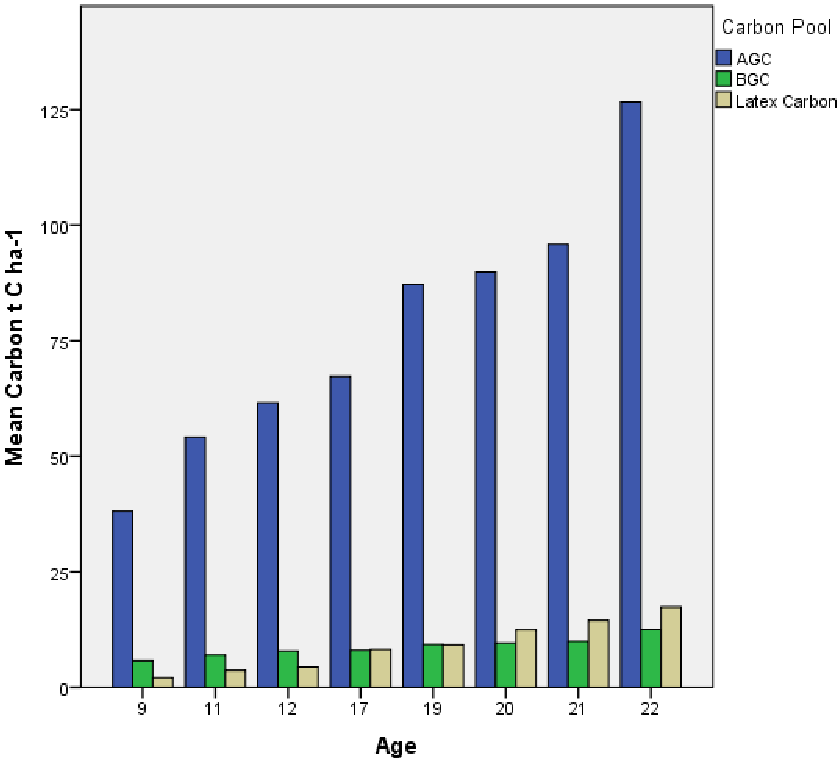

Figure 13: Comparison of carbon from different carbon pools (AGC, BGC and Latex) for different ages

From Figure 13, the AGC towers high above the BGC and Latex carbon content across all the ages. The BGC is higher than the Latex carbon at the initial ages of 9 to 12 years, however, as the stand age increases, the carbon from the latex begins to increase more than BGC from age 17 and above. The differences in carbon among the 3 pools at age 9 are 82.91%, 12.56% and 4.53% respectively for AGC, BGC and latex carbon. At age 17 AGC recorded 80.56% whilst BGC and Latex carbon recorded 9.59% and 9.85% indicating that aboveground carbon was still high, whilst latex carbon hand slightly overtaken BGC by 0.26%. By age 22 the sequestered carbon for AGC, BGC and Latex carbon recorded 80.93%, 7.97% and 11.1% respectively which meant that AGC was still higher than BGC and Latex with a difference of 72.96% and 69.83%. Latex carbon which was less than BGC by 8.03% at age 9 is 3.13% higher at age 22.

A Shapiro Wilk's normality F (75) = 0.748, p< 0.05 showed that the distribution was not normal (Appendix 12). A Kruskal Wallis test (Appendix 13) for the differences in carbon pools revealed a statistically significant difference among the three carbon pools, Chi-Square (3, N = 75) = 49.436, p = .000. Aboveground carbon ranked highest (Mean=63), latex carbon ranked second highest (Mean=26.44), with belowground carbon assuming the third rank (Mean=24.56).

Post-hoc comparisons whilst controlling for the Bonferroni effect (Appendix 14) indicated that there was significant difference between aboveground carbon and belowground carbon Chi-Square (1, N = 25) = 36.766, p = .000; r = 0.75 which represents a 75% strong effect size. The same significant difference was recorded between aboveground carbon and latex carbon content. On the contrary, there was no significant difference between latex carbon content and belowground content as the results showed Chi-Square (1, N = 25) = 0.208, p = 0.648; r = 0.004 which represents a smaller effect size of 4%.

4.3. Objective 3: To analyze the relationship between Google Earth derived canopy projected area and diameter at breast height

4.3.1. Multi-resolution segmentation

Results of the multi-resolution segmentation, cloud and shadow masking, morphology and watershed transformation is shown in Figure 14. The scale parameter set was 20 and 0.5 for both shape and compactness as obtained from the ESP tool.

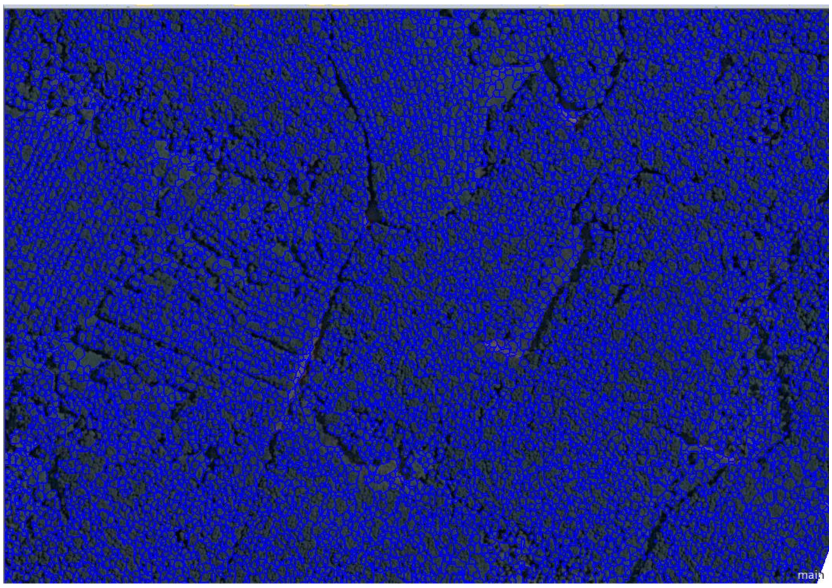

Figure 14: Tree crown delineation using Multi-Resolution Segmentation

4.3.2. Accuracy assessment

The segmentation accuracy was assessed using the goodness of fit "D" value computed from the results of over-segmentation and under-segmentation. Out of total of 190 manually delineated tree crowns, 102 trees were found to have a 1 to 1 matching with segmented crowns on the Google Earth images were used. For the whole study area over- segmentation value was 0.43 (43% error) and the under-segmentation was 0.32 (32% error) with the D-Value computed as 0.38 (38% error) which means that the segmentation accuracy is 62%. Table 9 below a summary of the accuracy assessment. This also summary shows that over-segmentation is greater than under-segmentation.

Table 9: Segmentation accuracy

	Total Reference Polygons	Total 1:1 Match	Over-Segmentation	Under-Segmentation	D-value
1:1	190	102			
Goodness of fit			0.43	0.32	0.38
Total accuracy		53.70%			62%

Figure 15 shows an overlay of reference polygons for segmentation accuracy assessment in red polygons on top of the and Google Earth image.

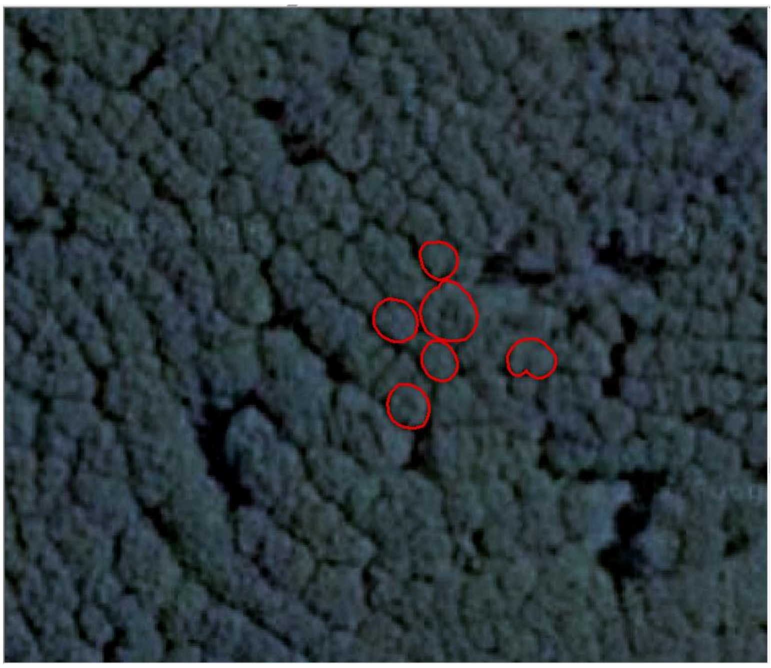

Figure 15: Shows an overlay of the manual crown delineation.

4.3.3. Relationship between Google Earth derived canopy projection area and diameter at breast height

To determine the extent to which DBH values can be predicted using Google Earth derived image object segments, a non-linear relationship between the Google Earth derived CPA and DBH was established. The models were developed using the trees spotted in the field and the trees spotted in the image. Figure 16 shows linear and non-linear relationships that were established between the two variables (DBH as dependent variable and Google Earth derived CPA as independent variable).

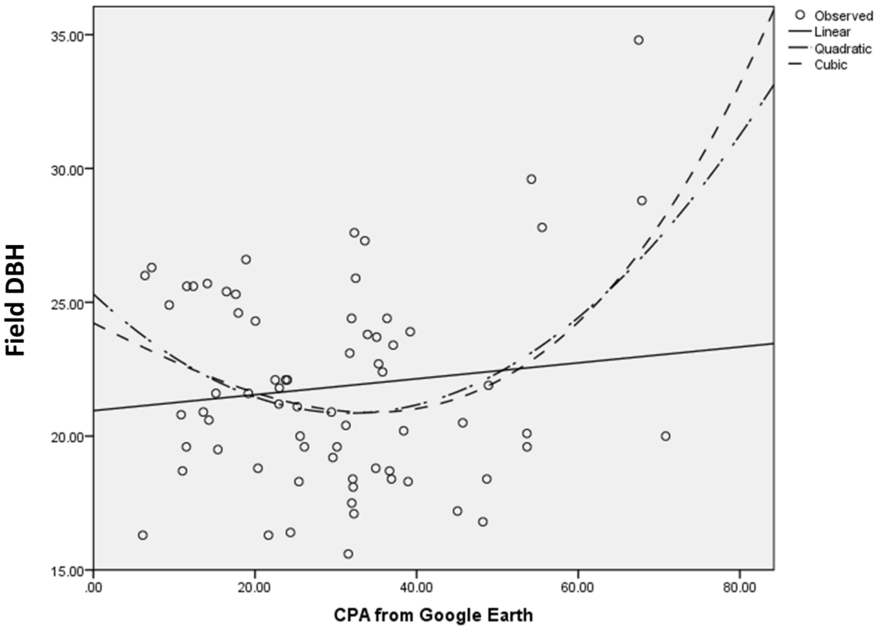

Figure 16: Relationship between DBH from field data and Google Earth derived CPA

The linear, quadratic and cubic models were evaluated and reported in Table 10. From the models developed, the quadratic model had an RMSE value 0.15 and a mean absolute percentage error (MAPE) of 0.159. The cubic model reported a higher RMSE value of 0.28 and a MAPE of 0.161 with the linear model presenting the highest RMSE value of 1.19 and a MAPE of 0.421. The linear, quadratic and cubic models recorded correlation co-efficient values of 0.119, 0.370 and 0.373 and R^2 values of 0.0014, 0.137 and 0.139, respectively indicating a weak correction between variables.

Table 10: Models for estimating DBH

Model Type	Model equation	r	R^2	RMSE	MAPE	p-value
Linear	DHB = 0.30*CPA +20.952	0.119	0.014	1.190	0.421	0.327
Quadratic	DBH =0.004*CPA^2+-0.281*CPA+25.309	0.370	0.137	0.150	0.159	0.007
Cubic	DHB =0.00004 *CPA^3 + 0.0002 *CPA^2 - 0.150 *CPA + 24.225	0.373	0.139	0.280	0.161	0.019

5. DISCUSSION

5.1. Objective 1: To determine the differences in carbon from latex for different ages categories.

The estimation of carbon sequestered by rubber plantations primarily have included aboveground and belowground carbon pools. Due to the omission of the carbon content from the latex, sequestered carbon is not completely accounted for, thus, quantifying the latex from the carbon is pertinent (Blagodatsky et al., 2016). Variation in the production of latex increases as the age of the rubber plantation increases (G Schroth et al., 2004), which makes it equally vital to assess whether carbon from latex is constant or different across different age stands.

The premier objective of this study was to determine the differences in the carbon from latex across the different age categories whilst hypothesizing that significant differences exist among the different age categories. The purpose is to evaluate the importance of age in latex carbon sequestration and how it affects carbon estimation for rubber plantations in general.

The differences in carbon from latex (t C ha^{-1}) increases across different age classes for rubber plantations (Table 6), as a tree stand grows older, the carbon from the latex increases. Tapping frequency of latex observed from the field visit for this study was higher for the older rubber trees than for the younger rubber trees, hence this explains the differences in latex carbon content across the different ages. The differences are significant for latex produced from rubber tree stands that are above 20 years and the latex from rubber tree stands that are below the age class of 20. Nguyen (2013) observed that, optimum latex production (kg) occurs after 20 years therefore this accounted for the significant differences observed in latex carbon pool at age 20 and above compared to ages below 20 years. Rubber tree stands that are above 20 years old can be significantly different from each other (Table 7), however, rubber tree stands below 20 years do not show any significant difference from each other with respect to the latex carbon content they produce.

The hypothesis that there exists significant differences in carbon from latex across different age categorisations cannot be rejected for latex carbon obtained from rubber stands that are above 20 years. On the contrary, the hypothesis can be rejected for latex carbon obtained from rubber stands that are below 20 years since they exhibit no significant difference. This follows that a complete carbon assessment comprising aboveground, belowground and latex as carbon pools for rubber plantations above 20 years will have the carbon contribution from latex significantly higher than plantations below 20 years.

In the work of Blagodatsky et al., (2016) on the uncertainties of carbon balance on rubber plantations, it was suggested that carbon from latex increases as the with age even up until age 25. Petsri et al., (2013) opined that carbon from latex continually increased with age as the productivity of latex increases with age but observed that latex production begins to decline after 24-25 years where latex carbon also declines. The findings of the aforementioned authors are no different from the findings produced by this study which confirms that latex production increases with age, and further causes the carbon from the latex to be high for latex older tree stands, especially those above 20 years.

The latex carbon content is influenced by the dry rubber content (DRC) fraction inherent in the latex as the DRC is mainly made up of hydrocarbons (Jayanthy & Sankaranarayanan, 2005). The higher the DRC the higher the carbon content to be contained in the latex. Therefore, with a constant DRC fraction the carbon from the latex will increase as the tapping and production frequency increases, hence the more latex is produced, the higher the carbon to be realised. This explains the differences in carbon from latex across the different ages and the higher carbon values obtained from latex produced by older rubber tree stands.

5.2. Objective 2: To compare the differences in the contribution of latex, aboveground and belowground carbon pools to carbon sequestration.

As part of plant photosynthesis, rubber trees sequester carbon into pools such as aboveground biomass, belowground biomass and latex (Munasinghe et al., 2014). To further enhance carbon accounting for rubber plantations and investigate the contribution of latex to carbon sequestration, the carbon accumulated and stored in the aboveground, belowground and latex were compared. Aboveground and belowground carbon pools are traditionally accepted pools in carbon accounting, however, latex is not, therefore the comparison was necessary to help expand knowledge on latex carbon and the possibility of its inclusion to the carbon pools.

The findings of this study on the comparison of aboveground carbon (AGC), belowground carbon (BGC) and latex carbon indicated that as the rubber tree grows and accumulates more age in years, the carbon pools also accumulate more carbon (Figure 13). The differences in sequestered carbon by the pools indicated that aboveground carbon pool is significantly associated with higher amounts of carbon relative to BGC and latex carbon across different age categorisations. The differences in AGC in comparison to both BGC and latex carbon content widens with age (Table 8). Belowground carbon on the other hand and carbon from latex comparatively do not have significant differences in sequestered carbon. Carbon from belowground biomass was found by this study to be relatively higher than carbon from latex at the age of 9 years when latex carbon is low, however, carbon from latex increases above carbon from the belowground as the age of the plantation increases.

The hypothesis that there exists significant differences in contribution of latex, aboveground and belowground carbon pools to carbon sequestration was partially met by this study. Aboveground carbon is significantly higher than both belowground and latex carbon, but there is no significant difference between the belowground carbon and the latex carbon.

The variations in the carbon sequestered by the various pools could be attributed to the fact that various methods used in the carbon computation for the aboveground and belowground carbon on one hand and the latex carbon on the other hand. Nonetheless, the findings made by this research that aboveground carbon is highest in terms of sequestered carbon relative to all the other pools is consistent with the findings made by Maggiotto et al., (2014). Aboveground carbon has higher biomass relative to the belowground and latex pools. The decrease in root to shoot ratio as the age increases is no different from the findings of (Wauters et al., 2008; Petsri et al., 2013) who reported that shoot to root ratio decreased with age. Petsri et al., (2013) indicated that as the carbon content increased in the biomass of the rubber tree the latex carbon equally increased yet there existed significant differences between the carbon sequestered by the living tree and the carbon sequestered by the latex. This supports the findings made by this study that although carbon content from this study is no different from carbon from the belowground carbon pool, aboveground carbon by far remains the highest carbon pool. Additionally, in a presentation of the components of carbon budget in a review of carbon balance on rubber plantations, Blagodatsky et al., (2016) reported that as AGC increased, latex carbon increased but belowground carbon was on the decline. Thus, carbon from latex can be considered as a pool due to its significant levels comparable to belowground carbon, however, aboveground carbon still holds the greatest component of sequestered carbon for rubber plantations.

5.3. Objective 3: To analyze the relationship between Google Earth derived canopy projected area and diameter at breast height

Segmentation results were based on objects that exhibited 50% one to one matching between image object segments and manually delineated crowns (Zhan et al., 2005). The segmentation process for the Google Earth Imagery yielded 43% over-segmentation error for the and an under-segmentation error of 32% with overall Goodness of fit at 62%. The segmentation accuracy does not differ much from that of Bautista (2012) who obtained 62% accuracy in segmentation of optical Geo-eye Image although the objects he was looking at were primary forests with larger tree crown. The author obtained over segmentation error of 48% of which was higher than in the case of the Google Earth Imagery segments although under segmentation error was lower than the Google Earth Imagery segments at 23%. Accordingly, Karna et al., (2015) obtained segmentation accuracy of 67% on WorldView-2 which is equally not too different from the overall segmentation accuracy obtained for the Google Earth Imagery segmentation from process.

However, there are differences in the correlation coefficients and the coefficients of determination in the models developed in spite of the similar segmentation accuracies. The results of the modelling from the Google Earth Imagery segmentation indicated that none of the three models (linear, quadratic, and cubic) could strongly predict DBH. The correlation coefficients were weak as the best correlation coefficient was exhibited by the quadratic model which had an r value of 0.37 and the coefficients of determination at best was 0.137. Karna et al., (2015) and Bautista (2012) reported an r of 0.871 and 0.72 and an R^2 of 0.759 and 0.41 showing stronger relationships between the various variables in their models.

The weak correlation between the DBH and the Google Earth imagery derived CPA can be attributed to the highly dense nature of the rubber tree crowns coupled with the poor spectral resolution to clearly delineate the rubber tree crowns automatically (Hu et al., 2013). Vegetation exhibit higher reflectance in the near infrared portion which is absent from the Google Earth Imagery therefore dense crowns of the same age and similar characteristics could not be clearly distinguished from the google image (Li & Fox, 2012).

According to Bluman (2012), a correlation coefficient of 1 and -1 indicates a strong correlation hence as the correlation values decreases towards 0, a weak correlational effect exists among variables under study. The author further posits that coefficient of determination describes the amount of variation in predicted variables that models can explain. In this context the models developed from the Google Earth derived CPA could not adequately account for more than 80% of the variation in the DBH. Therefore, based on this study, Google Earth derived segments cannot be used to predict DBH of rubber plantations with dense canopy cover.

6. CONCLUSIONS AND RECOMENDATIONS

6.1. Conclusion

Although rubber plantations are established for economic reasons, the environmental contribution they make by way of carbon sequestration needs to be holistically assessed and understood. Accounting for the carbon sequestered by the latex helps to reduce the uncertainties related to accounting for sequestered carbon for rubber plantations. From the findings made by this study, the carbon in latex from rubber plantations was significantly equal to the carbon in the belowground biomass, however, there was a significant difference between the carbon sequestered by the latex and carbon sequestered by aboveground biomass. On the other hand, using the multiresolution object based segmentation, Google Earth imagery was found to be unsuitable to estimate the diameter at breast height of rubber plantations with dense canopy cover.

How does carbon from latex differ across different age categories?

Carbon from latex increased as more latex is produced by the rubber trees with are older. The results indicated that latex carbon from rubber stands above 20 years of age were significantly higher than latex from rubber stands that are below 20 years at $p=0.000$.

How significant are the differences in the latex, aboveground and belowground carbon pools?

Aboveground was significantly higher in terms of sequestered carbon with an overall effect size of 75% at $p=0.000$ relative to the remaining carbon pools. However, no significant difference was recorded for belowground carbon and latex carbon as their effect size was of 4% for each at $p= 0.648$.

How strong is the relationship between Google Earth derived Canopy Projection Area and Diameter at Breast Height?

There is no relationship between Google Earth derived image object segments and field measured diameter at breast height. As the linear, quadratic and cubic models could only account for 1.4%, 13.7% and 13.9% of the variation in the diameter at breast height.

6.2. Recommendation and Limitation

The multi-resolution segmentation process performed on the Google Earth could not lead to the development of accurate models to establish a relationship between the image object segments and field collected DBH. Further exploration should be conducted to focus on building models for each age compartment found within rubber plantations landscape, as well as alternative segmentation algorithms that can perform better than the multi-resolution segmentation algorithm.

LIST OF REFERENCES

Aalde, H., Gonzalez, P., Gytarsky, M., Krug, T., Kurz, W. A., Ogle, S., … Somogoyi, Z. (2006). Forest Land. In *2006 IPCC Guidelines for National Greenhouse Gas Inventories* (Vol. 4, p. 4.1-4.83). Retrieved from http://www.ipcc-nggip.iges.or.jp/public/2006gl/pdf/4_Volume4/V4_04_Ch4_Forest_Land.pdf

AfDB/OECD/UNDP. (2015). *African Economic Outlook 2015. OECD Publishing*. Paris: OECD Publishing. https://doi.org/10.1787/aeo-2015-en

Almeer, M. H. (2012). Vegetation Extraction from Free Google Earth Images of Deserts Using a Robust BPNN Approach in HSV Space. *International Journal of Advanced Research in Computer and Communication Engineering*, *1*(3), 134–140.

Arhin, K. (1980). The Economic and Social Significance of Rubber Production and Exchange on the Gold and Ivory Coasts , 1880-1900 (Signification économique et sociale de la production et du commerce du caoutchouc en Côte d'Ivoire et Côte de l'Or, 1880-1900). *Cahiers D'Etudes Africaines*, *20*(77/78), 49–62. Retrieved from http://www.jstor.org/stable/4391679

Assefa, G., Mengistu, T., Getu, Z., & Zewdie, S. (2013). *Training manual on: Forest carbon pools and carbon stock assessment in the context of SFM and REDD+*.

Bakx, W., Janssen, L., Schetselaar, E., Tempfli, K., Tolpekin, V., & Westinga, E. (2013). Chapter 06 - Image Analysis. In *The core of GIScience a process based approach.* (pp. 205–225). Enschede: Faculty of Geo-Information Science and Earth Observation (ITC) of the University of Twente. Retrieved from https://issuu.com/itc-utwente/docs/corebook2013_06_imageanalysis

Bank, W. (2005). Carbon Finance at the World Bank. Retrieved August 14, 2016, from papers3://publication/uuid/FDFED53C-271D-408B-A143-8FE02B549690

Bautista, L. A. A. (2012). *Biomass Carbon Estimation and Mapping in the Subtropical Forest of Chitwan, Nepal : a comparison between VHR geo-eye satellite images and airborne LIDAR data*. University of Twente, Faculty of Geo-Information and Earth Observation (ITC). (MSc. Thesis). Retrieved from http://www.itc.nl/library/papers_2012/msc/nrm/lopezbautista.pdf

Blagodatsky, S., Xu, J., & Cadisch, G. (2016). Carbon balance of rubber (Hevea brasiliensis) plantations: A review of uncertainties at plot, landscape and production level. *Agriculture, Ecosystems and Environment*, *221*, 8–19. https://doi.org/10.1016/j.agee.2016.01.025

Blinn, C., Zamora, D., & Taylor, E. (2013). Climate Change and Carbon Sequestration [Image]). Retrieved February 8, 2017, from http://articles.extension.org/pages/26786/climate-change-and-carbon-sequestration

Bluman, A. G. (2012). *Elementary Statistics A Step by Step Approach. McGraw Hill* (8th edn). New York, NY: McGraw-Hill. https://doi.org/10.1007/s13398-014-0173-7.2

Brown, S. (2002). Measuring carbon in forests: current status and future challenges. *Environmental Pollution*, *116*(3), 363–372. https://doi.org/10.1016/S0269-7491(01)00212-3

Charoenjit, K., Zuddas, P., Allemand, P., Pattanakiat, S., & Pachana, K. (2015, March 19). *Estimation of biomass and carbon stock in Para rubber plantations using object-based classification from Thaichote satellite data in Eastern Thailand. Journal of Applied Remote Sensing*. Universit´e Pierre et Marie Curie. Paris. https://doi.org/10.1117/1.JRS.9.096072

Chen, B., Li, X., Xiao, X., Zhao, B., Dong, J., Kou, W., … Xie, G. (2016). Mapping tropical forests and deciduous rubber plantations in Hainan Island, China by integrating PALSAR 25-m and multi-temporal Landsat images. *International Journal of Applied Earth Observation and Geoinformation*, *50*, 117–130. https://doi.org/10.1016/j.jag.2016.03.011

Concato, J., Peduzzi, P., Holford, T. R., & Feinstein, A. R. (1995). Importance of events per independent variable in proportional hazards analysis I. Background, goals, and general strategy. *Journal of Clinical Epidemiology*, *48*(12), 1495–1501. https://doi.org/10.1016/0895-4356(95)00510-2

Danso-Manu, M., Poku, E. N., & Fayorsey, C. K. (2013). *2010 Population and Housing Census: Regional Analytical Report - Western Region*. Retrieved from http://www.statsghana.gov.gh/docfiles/2010phc/2010_PHC_Regional_Analytical_Reports_Western_Region.pdf

Derivaux, S., Forestier, G., Wemmert, C., & Lefèvre, S. (2010). Supervised image segmentation using watershed transform, fuzzy classification and evolutionary computation. *Pattern Recognition Letters*, *31*(15), 2364–2374. https://doi.org/10.1016/j.patrec.2010.07.007

Drăguţ, L., Csillik, O., Eisank, C., & Tiede, D. (2014). Automated parameterisation for multi-scale image segmentation on multiple layers. *ISPRS Journal of Photogrammetry and Remote Sensing*, *88*, 119–127. https://doi.org/10.1016/j.isprsjprs.2013.11.018

Dră guţ, L., Tiede, D., & Levick, S. R. (2010). ESP: a tool to estimate scale parameter for multiresolution image segmentation of remotely sensed data. *International Journal of Geographical Information Science*, *24*(6), 859–871. https://doi.org/10.1080/13658810903174803

Driessen, P., Deckers, J., & Spaargaren, O. (2001). *Lecture Notes on the major Soils of the world. World Soil Resources Reports*. Rome. https://doi.org/10.1136/gut.27.11.1400-b

du Prel, J.-B., Röhrig, B., Hommel, G., & Blettner, M. (2010). Choosing statistical tests: Part 12 of a series on evaluation of scientific publications. *Deutsches Ärzteblatt International*, *107*(19), 343–348. https://doi.org/10.3238/arztebl.2010.0343

Egbe, A. E., Tabot, P. T., Fonge, B. A., & Bechem, E. (2012). Simulation of the impacts of three management regimes on carbon sinks in rubber and oil palm plantation ecosystems of South- Western Cameroon. *Journal of Ecology and the Natural Environment*, *4*(6), 154–162. https://doi.org/10.5897/JENE11.146

ESA. (2012). *Report for Mission Selection: Biomass, ESA SP-1324/1 (3 volume series), European Space Agency*. Noordwijk, The Netherlands. Retrieved from http://esamultimedia.esa.int/docs/EarthObservation/SP1324-1_BIOMASSr.pdf

FAO. (2010). *Global Forest Resources Assessment 2010. America* (Vol. 147). Rome. https://doi.org/ISBN 978-92-5-106654-6

Gao, H., Siu, W. C., & Hou, C. H. (2001). Improved techniques for automatic image segmentation. *IEEE Transactions on Circuits and Systems for Video Technology*, *11*(12), 1273–1280. https://doi.org/10.1109/76.974681

Ghana Statistical Service. (2012). *2010 Population and Housing Census Ghana Statistical Service 2010 Population and Housing Census (PHC)*. Retrieved from http://www.statsghana.gov.gh/docfiles/2010phc/2010_POPULATION_AND_HOUSING_CENSUS_FINAL_RESULTS.pdf

Gibbs, H. K., Brown, S., Niles, J. O., & Foley, J. A. (2007). Monitoring and estimating tropical forest carbon stocks: making REDD a reality. *Environmental Research Letters*, *2*(4), 45023. https://doi.org/10.1088/1748-9326/2/4/045023

Goetz, S., Baccini, A., Laporte, N., Johns, T., Walker, W., Kellndorfer, J., … Sun, M. (2009). Mapping and monitoring carbon stocks with satellite observations: a comparison of methods. *Carbon Balance and Management*, *4*(1), 2. https://doi.org/10.1186/1750-0680-4-2

Green, S. B., & Salkind, N. J. (2008). *Using SPSS for Windows and Macintosh : analyzing and understanding data* (5th ed.). Kansas: Pearson/Prentice Hall. Retrieved from https://www.pearsonhighered.com/product/Green-Using-SPSS-for-Windows-and-Macintosh-Analyzing-and-Understanding-Data-5th-Edition/9780131890251.html

Greenacre, M., & Primicerio, R. (2013). Multivariate Data in Environmental Science. In *Multivariate Analysis of Ecological Data* (p. 20). Bilbao: Fundación BBVA.

GREL. (n.d.). History. Retrieved July 28, 2016, from http://grelgh.com/history/

Gschwantner, T., Schadauer, K., Vidal, C., Lanz, A., Tomppo, E., di Cosmo, L., … Lawrence, M. (2009). Common tree definitions for national forest inventories in Europe. *Silva Fennica*, *43*(2), 303–321. https://doi.org/10.14214/sf.463

Hay, G. J., Castilla, G., Wulder, M. A., & Ruiz, J. R. (2005). An automated object-based approach for the multiscale image segmentation of forest scenes. *International Journal of Applied Earth Observation and Geoinformation*, *7*(4), 339–359. https://doi.org/10.1016/j.jag.2005.06.005

Hu, Q., Wu, W., Xia, T., Yu, Q., Yang, P., Li, Z., & Song, Q. (2013). Exploring the use of google earth imagery and object-based methods in land use/cover mapping. *Remote Sensing*, *5*(11), 6026–6042. https://doi.org/10.3390/rs5116026

Hunt, C. A. G. (2009). Measuring the Carbon in Forest Sinks. In *Carbon Sinks and Climate Change, Forests In The Fight Against Global Warming* (pp. 121–140). Cheltenham: Edward Elgar Publishing Limited. https://doi.org/10.1080/10549811.2011.530937

Husch, B., Beers, T. W., & Kershaw, J. A. (2003). Non Timber Forest Vegetation Parmeters. In *Forest Mensuration* (4th edn, pp. 229–244). New York: John Wiley & Sons Inc.

Ingvaldsen, J. E., & Gulla, J. A. (2015). Summary for Policymakers. In Intergovernmental Panel on Climate Change (Ed.), *Climate Change 2013 - The Physical Science Basis* (Vol. 1542, pp. 1–30). Cambridge:

Cambridge University Press. https://doi.org/10.1017/CBO9781107415324.004

IPCC. (2014). *Climate Change 2014 :Synthesis Report. Contribution of Working Groups I, II and III to the Fifth Assessment Report of the Intergovernmental Panel on Climate Change [Core Writing Team, R.K. Pachauri and L.A. Meyer (eds.)]*. IPCC, Geneva.

Jayanthy, T., & Sankaranarayanan, P. E. (2005). Measurement of Dry Rubber Content in Latex Using Microwave Technique. *Measurement Science Review*, *5*(3), 50–54. Retrieved from http://www.measurement.sk/2005/S3/Jayanthy.pdf

Joseph, G. (2005). Data Analysis. In G. Joseph (Ed.), *Fundamentals of Remote Sensing* (2nd Ed., pp. 319–348). India: University Press.

Karna, Y. K., Hussin, Y. A., Gilani, H., Bronsveld, M. C., Murthy, M. S. R., Qamer, F. M., … Baniya, C. B. (2015). Integration of WorldView-2 and airborne LiDAR data for tree species level carbon stock mapping in Kayar Khola watershed, Nepal. *International Journal of Applied Earth Observation and Geoinformation*, *38*, 280–291. https://doi.org/10.1016/j.jag.2015.01.011

Khalid, K. B. I. N. (1991). Determination of Dry Rubber Content (DRC) of Hevea Rubber Latex by Microwave Drying, *67*(l), 65–67.

Kongsager, R., Napier, J., & Mertz, O. (2013). The carbon sequestration potential of tree crop plantations. *Mitigation and Adaptation Strategies for Global Change*, *18*(8), 1197–1213. https://doi.org/10.1007/s11027-012-9417-z

Kottek, M., Grieser, J., Beck, C., Rudolf, B., & Rubel, F. (2006). World Map of the Köppen-Geiger climate classification updated. *Meteorologische Zeitschrift*, *15*(3), 259–263. https://doi.org/10.1127/0941-2948/2006/0130

Li, Z., & Fox, J. M. (2011). Integrating Mahalanobis typicalities with a neural network for rubber distribution mapping. *Remote Sensing Letters*, *2*(2), 157–166. https://doi.org/10.1080/01431161.2010.505589

Li, Z., & Fox, J. M. (2012). Mapping rubber tree growth in mainland Southeast Asia using time-series MODIS 250 m NDVI and statistical data. *Applied Geography*, *32*(2), 420–432. https://doi.org/10.1016/j.apgeog.2011.06.018

Liu, G., & Han, S. (2009). Long-term forest management and timely transfer of carbon into wood products help reduce atmospheric carbon. *Ecological Modelling*, *220*(13–14), 1719–1723. https://doi.org/10.1016/j.ecolmodel.2009.04.005

Lu, D. (2006). The potential and challenge of remote sensing- based biomass estimation. *International Journal of Remote Sensing*, *27*(7), 1297–1328. https://doi.org/10.1080/01431160500486732

Maggiotto, S. R., Oliveira, D. De, Marur, C. J., Stivari, S. M. S., Leclerc, M., Wagner-Riddle, C., … Wagner-Riddle, C. (2014). Potential carbon sequestration in rubber tree plantations in the northwestern region of the Paraná State, Brazil. *Acta Scientiarum - Agronomy*, *36*(2), 239–245. https://doi.org/10.4025/actasciagron.v36i2.17404

Mbabazi, J. (2011). Ecosystem Goods and Services from Plantation Forests. *International Journal of Environmental Studies*, *68*(2), 249–250. https://doi.org/10.1080/00207233.2011.552230

Moller, M., Lymburner, L., & Volk, M. (2007). The comparison index : A tool for assessing the accuracy of image segmentation, *9*, 311–321. https://doi.org/10.1016/j.jag.2006.10.002

Munasinghe, E. S., Rodrigo, V. H. L., & Gunawarden, U. A. D. P. (2014). Modus Operandi in Asessing Biomass and Carbon in Rubber Plantations Under Varying Climatic Conditions. *Experimental Agriculture*, *50*(1), 40–58. https://doi.org/10.1017/S0014479713000410

NASA. (n.d.). A blanket around the Earth [Image]. Retrieved February 23, 2017, from https://climate.nasa.gov/causes/

Nguyen, B. T. (2013). Large-scale altitudinal gradient of natural rubber production in Vietnam. *Industrial Crops and Products*, *41*, 31–40. https://doi.org/10.1016/j.indcrop.2012.04.006

Nizami, S. M., Yiping, Z., Liqing, S., Zhao, W., Zhang, X., & Wang, S. (2014). Managing carbon sinks in rubber (Hevea brasilensis) Plantation by changing rotation length in SW China. *PLoS ONE*, *9*(12), 1–9. https://doi.org/10.1371/journal.pone.0115234

Nordh, N.-E., & Verwijst, T. (2004). Above-ground biomass assessments and first cutting cycle production in willow (Salix sp.) coppice—a comparison between destructive and non-destructive methods. *Biomass and Bioenergy*, *27*(1), 1–8. https://doi.org/10.1016/j.biombioe.2003.10.007

Omair, A. (2014). Sample size estimation and sampling techniques for selecting a representative sample. *Journal of Health Specialties*, *2*(4), 142. https://doi.org/10.4103/1658-600X.142783

Peduzzi, P., Concato, J., Feinstein, A. R., & Holford, T. R. (1995). Importance of events per independent variable in proportional hazards regression analysis II. Accuracy and precision of regression estimates. *Journal of Clinical Epidemiology*, *48*(12), 1503–1510. https://doi.org/10.1016/0895-4356(95)00048-8

Petsri, S., Chidthaisong, A., Pumijumnong, N., & Wachrinrat, C. (2013). Greenhouse gas emissions and carbon stock changes in rubber tree plantations in Thailand from 1990 to 2004. *Journal of Cleaner Production*, *52*, 61–70. https://doi.org/10.1016/j.jclepro.2013.02.003

Ploton, P., Pélissier, R., Proisy, C., Flavenot, T., Barbier, N., Rai, S. N., & Couteron, P. (2012). Assessing aboveground tropical forest biomass using Google Earth canopy images. *Ecological Applications*, *22*(3), 993–1003. https://doi.org/10.1890/11-1606.1

Qureshi, A., Pariva, Badola, R., & Hussain, S. A. (2012). A review of protocols used for assessment of carbon stock in forested landscapes. *Environmental Science & Policy*, *16*, 81–89. https://doi.org/10.1016/j.envsci.2011.11.001

Ratnasingam, J., Thiruselvam, K., & Ioras, F. (2016). The potential of rubber and acacia plantations for forest carbon stocks in Malaysia. *International Forestry Review*, *18*(1), 68–77. https://doi.org/10.1505/146554816818206140

Razali, N. M., & Wah, Y. B. (2011). Power comparisons of Shapiro-Wilk, Kolmogorov-Smirnov, Lilliefors and Anderson-Darling tests. *Journal of Statistical Modeling and Analytics*, *2*(1), 21–33. Retrieved from http://www.de.ufpb.br/~ulisses/disciplinas/normality_tests_comparison.pdf

Rejaur Rahman, M., & Saha, S. K. (2008). Multi-resolution segmentation for object-based classification and accuracy assessment of land use/land cover classification using remotely sensed data. *Journal of the Indian Society of Remote Sensing*, *36*(2), 189–201. https://doi.org/10.1007/s12524-008-0020-4

Rejikumar, R., & Philip, J. (2010). Estimation of dry rubber content in natural rubber latex by differential scanning calorimetry. *Journal of Thermal Analysis and Calorimetry*, *101*(3), 1047–1050. https://doi.org/10.1007/s10973-010-0716-x

Rose, K., & Steinbuchel, A. (2005). Biodegradation of Natural Rubber and Related Compounds: Recent Insights into a Hardly Understood Catabolic Capability of Microorganisms. *Applied and Environmental Microbiology*, *71*(6), 2803–2812. https://doi.org/10.1128/AEM.71.6.2803-2812.2005

Rozanda, N. E., Ismail, M., & Permana, I. (2015). Segmentation google earth imagery using K-means clustering and normalized RGB color space. In *Smart Innovation, Systems and Technologies* (Vol. 31, pp. 375–386). https://doi.org/10.1007/978-81-322-2205-7_36

Schroth, G., Coutinho, P., Moraes, V. H. F., & Albernaz, A. L. (2003). Rubber agroforests at the Tapajós river, Brazilian Amazon - Environmentally benign land use systems in an old forest frontier region. *Agriculture, Ecosystems and Environment*, *97*(1–3), 151–165. https://doi.org/10.1016/S0167-8809(03)00116-6

Schroth, G., Moraes, V. H. F., & Da Mota, M. S. S. (2004). Increasing the profitability of traditional, planted rubber agroforests at the Tapajos river, Brazilian Amazon. *Agriculture, Ecosystems and Environment*, *102*(3), 319–339. https://doi.org/10.1016/j.agee.2003.09.001

Shafri, H. Z. M., Hamdan, N., & Saripan, M. I. (2011). Semi-automatic detection and counting of oil palm trees from high spatial resolution airborne imagery. *International Journal of Remote Sensing*, *32*(8), 2095–2115. https://doi.org/10.1080/01431161003662928

Shimano, K. (1997). Analysis of the relationship between DBH and crown projection area using a new model. *Journal of Forest Research*, *2*(4), 237–242. https://doi.org/10.1007/BF02348322

Song, C., Dickinson, M. B., Su, L., Zhang, S., & Yaussey, D. (2010). Estimating average tree crown size using spatial information from Ikonos and QuickBird images: Across-sensor and across-site comparisons. *Remote Sensing of Environment*, *114*(5), 1099–1107. https://doi.org/10.1016/j.rse.2009.12.022

Srivastava, N. (2008). IPCC Guidelines and REDD Monitoring and Verification. In *Expert Consultation on National Forest Monitoring and Assessment (NFMA): Meeting Evolving Needs*. Rome. Retrieved from http://www.fao.org/forestry/16663-0d866304c10b8384d90eb4fdef89867df.pdf

Sundquist, E., Burruss, R., Faulkner, S., Gleason, R., Harden, J., Kharaka, Y., … Waldrop, M. (2008). *Carbon Sequestration to Mitigate Climate Change*. US. Retrieved from https://blackboard.utwente.nl/bbcswebdav/pid-943266-dt-content-rid-2072979_2/courses/M16-NRS-100/CarbonFS%281%29_paper.pdf

Tan, Z., Yang, X., Ou, Z., Sun, H., Chen, H., Xi, G., & Application, R. S. (2006). The Extraction of Rubber Spatial Distributing Information in Hainan Province Based on FY -3A Satellite Data -, 25–29.

Tesema, M. A. (2015). Estimating and Mapping Aboveground Carbon Stocks in Cocoa Plantation Using

Worldview-2 Satellite Image and Lidar Data, 1–58.

Trimble. (2014). Segmentation Algorithms. In *eCognition ® Developer Reference Book* (pp. 35–39). Munchen: Trimble Germany GmbH.

Tsendbazar, N. (2011). *Object Based Image Aanalysis of Geo-eye VHR Data To Model Above Ground Carbon Stock in Himalayan Mid-Hill Forests, Nepal*. University of Twente, Faculty of Geo-Information and Earth Observation (ITC). (MSc. Thesis). Retrieved from http://www.itc.nl/Pub/Home/library/Academic_output/AcademicOutput.html?p=11&y=11&l=20

UN-REDD. (2013). About REDD+. Retrieved June 2, 2016, from http://www.un-redd.org/aboutredd/tabid/582/default.aspx

UNFCCC. (1997). Kyoto Protocol To The United Nations Framework Convention On Climate Change (pp. 1–20). Kyoto. Retrieved from http://unfccc.int/kyoto_protocol/items/2830.php

UNFCCC. (2015). *Measurements for Estimation of Carbon Stocks in Afforestation and Reforestation Project Activities under the Clean Development Mechanism: A Field Manual*. Retrieved from http://unfccc.int/resource/docs/publications/cdm_afforestation_field-manual_web.pdf

UNFCCC. (2016). REDD+: Forest reference emission levels. Retrieved June 1, 2016, from http://redd.unfccc.int/fact-sheets/forest-reference-emission-levels.html

Venkatachalam, P., Geetha, N., Sangeetha, P., & Thulaseedharan, A. (2013). Natural rubber producing plants : An overview. *African Journal of Biotechnology*, *12*(12), 1297–1310. https://doi.org/10.5897/AJBX12.016

Visser, V., Langdon, B., Pauchard, A., & Richardson, D. M. (2014). Unlocking the potential of Google Earth as a tool in invasion science. *Biological Invasions*, *16*(3), 513–534. https://doi.org/10.1007/s10530-013-0604-y

Watson, C. (2009). *Forest carbon accounting: overview and principles. Forest carbon accounting: overview and principles*. Retrieved from http://www.cabdirect.org/abstracts/20103082947.html

Wauters, J. B., Coudert, S., Grallien, E., Jonard, M., & Ponette, Q. (2008). Carbon stock in rubber tree plantations in Western Ghana and Mato Grosso (Brazil). *Forest Ecology and Management*, *255*(7), 2347–2361. https://doi.org/10.1016/j.foreco.2007.12.038

Werathirachot, R., Danwanichakul, P., Kongkaew, C., & Loykulnant, S. (2008). Water Soluble Chitosan as an Environment-Friendly Coagulant in Removal of Rubber Particles from Skim Rubber Latex. *Journal of Metals, Materials and Minerals*, *18*(2), 93–97. Retrieved from https://www.researchgate.net/publication/238079771_Water_Soluble_Chitosan_as_an_Environment-Friendly_Coagulant_in_Removal_of_Rubber_Particles_from_Skim_Rubber_Latex

Winter, S., & Brambach, F. (2011). Determination of a common forest life cycle assessment method for biodiversity evaluation. *Forest Ecology and Management*, *262*(12), 2120–2132. https://doi.org/10.1016/j.foreco.2011.07.036

Yang, X., Jiang, G. M., Luo, X., & Zheng, Z. (2012). Preliminary mapping of high-resolution rural population distribution based on imagery from Google Earth: A case study in the Lake Tai basin, eastern China. *Applied Geography*, *32*(2), 221–227. https://doi.org/10.1016/j.apgeog.2011.05.008

Yi, Z. F., Wong, G., Cannon, C. H., Xu, J., Becksch??fer, P., & Swetnam, R. D. (2014). Can carbon-trading schemes help to protect China's most diverse forest ecosystems? A case study from Xishuangbanna, Yunnan. *Land Use Policy*, *38*, 646–656. https://doi.org/10.1016/j.landusepol.2013.12.013

Yuen, J. Q., Fung, T., & Ziegler, A. D. (2016). Review of allometric equations for major land covers in SE Asia: Uncertainty and implications for above- and below-ground carbon estimates. *Forest Ecology and Management*, *360*, 323–340. https://doi.org/10.1016/j.foreco.2015.09.016

Yuen, J. Q., Ziegler, A. D., Webb, E. L., & Ryan, C. M. (2013). Uncertainty in below-ground carbon biomass for major land covers in Southeast Asia. *Forest Ecology and Management*, *310*, 915–926. https://doi.org/10.1016/j.foreco.2013.09.042

Zhan, Q., Molenaar, M., Tempfli, K., & Shi, W. (2005). Quality assessment for geo- spatial objects derived from remotely sensed data. *International Journal of Remote Sensing*, *26*(14), 2953–2974. https://doi.org/10.1080/01431160500057764

LIST OF APPENDICES

Appendix 1: Latex production data, year of planting and planted surface obtained from GREL (2016).

Block ID	Block	Size (Ha)	Year of Planting	Average_ Production per annum	Total Latex
1V3	V3	17.02	2005	26030.81	130154.07
1V4	V4	8.19	2005	15852.22	79261.09
1T5	T5	11.93	1999	17392.70	191319.70
1T6	T6	5.01	1999	6795.18	74746.95
1V5	V5	13.56	1999	17881.14	196692.56
1V6	V6	8.32	1999	12280.07	135080.78
1T3	T3	7.70	1997	6498.54	84480.98
1T4	T4	9.73	1997	13337.72	173390.39
1U5	U5	13.45	1999	16388.46	180273.02
1U6	U6	8.62	1999	12047.53	132522.79
1U2	U2	2.64	1997	5664.45	73637.81
1V2	V2	13.77	2005	25402.01	127010.03
1S1	S1	2.02	1997	11053.85	143700.01
1S2	S2	13.25	1997	17277.79	224611.25
1S5	S5	11.66	1996	15100.58	211408.18
1S6	S6	5.76	1996	6882.57	96356.04
1U3	U3	8.00	1997	7967.45	103576.80
1U4	U4	11.41	2005	11035.66	55178.29
1S7	S7	5.84	1996	12443.03	174202.36
1T7	T7	6.36	1996	10701.37	149819.13
1O9	O9	9.06	1995	16348.11	245221.64
1P9	P9	3.40	1996	6932.12	97049.62
1Q8	Q8	10.02	1996	17264.60	241704.38
1R7	R7	4.43	1996	9525.36	133355.03
1S3	S3	11.14	1997	13996.71	181957.29
1S4	S4	9.20	1997	10233.91	133040.83
1P1	P1	34.74	2007	45268.51	135805.53
1R4	R4	13.65	1996	24355.46	340976.38
1R5	R5	12.70	1996	21025.37	294355.24
1R6	R6	11.83	1996	17537.64	245526.89
1Q6	Q6	12.54	1996	17379.78	243316.97
1Q7	Q7	10.43	1996	17432.56	244055.85
1R3	R3	13.19	1996	21354.14	298958.00
1Q3	Q3	11.05	1996	21516.18	301226.55
1Q4	Q4	14.34	1996	29991.00	419873.97
1Q5	Q5	13.48	1996	23994.46	335922.38
1H1	H1	70.86	2005	111106.45	555532.23
1P6	P6	13.58	1996	26871.08	376195.07
1P7	P7	14.16	1996	25458.75	356422.56

1P8	P8	9.88	1996	15387.78	215428.90
1Q1	Q1	8.26	1997	9430.00	122589.97
1P3	P3	11.51	1996	23128.97	323805.57
1P4	P4	14.12	1996	29096.52	407351.24
1P5	P5	14.27	1996	24599.24	344389.31
1Q2	Q2	13.94	1996	21703.56	303849.79
1O6	O6	15.57	1995	21630.25	324453.73
1O7	O7	12.06	1995	23335.34	350030.04
1O1	O1	10.42	1996	11111.03	155554.40
1O2	O2	11.29	1996	14581.74	204144.42
1O3	O3	15.21	1995	29260.09	438901.33
1O4	O4	14.18	1995	27999.70	419995.47
1O5	O5	14.93	1995	30757.26	461358.83
1N8	N8	12.76	1995	23313.64	349704.54
1N9	N9	7.11	1995	15431.16	231467.40
1M1	M1	14.59	1996	22090.11	309261.58
1N5	N5	11.37	1995	24497.47	367462.07
1N6	N6	10.61	1995	20676.83	310152.46
1N7	N7	14.16	1995	24432.28	366484.14
1N2	N2	13.09	1996	19624.05	274736.66
1N3	N3	13.23	1995	18681.07	280216.11
1N4	N4	15.34	1995	25889.91	388348.70
1M5	M5	11.00	1995	18740.11	281101.64
1K5	K5	13.48	1994	27175.70	434811.15
1K6	K6	11.71	1994	24195.56	387128.97
1L6	L6	14.53	1994	13110.58	209769.21
1L1	L1	10.49	1996	13950.75	195310.48
1L2	L2	14.42	1995	18495.09	277426.35
1L7	L7	6.19	1994	15010.78	240172.44
1K4	K4	11.13	1995	18489.54	277343.04
1H4	H4	44.42	2005	43530.06	217650.29
1H2	H2	60.44	2005	69733.91	348669.55
1E3	E3	22.17	2004	36080.22	216481.32
1G3	G3	26.63	2005	35110.41	175552.03
1G4	G4	37.12	2005	50392.90	251964.51
1E1	E1	26.57	2004	37107.12	222642.70
1F2	F2	26.58	2005	42906.94	214534.70
1E4	E4	24.70	2004	36182.26	217093.56
1E5	E5	32.08	2004	51001.96	306011.77
1U1	U1	4.75	2005	6132.63	30663.16
1T2	T2	5.55	1997	7798.81	101384.48
1E2	E2	30.71	2004	37998.19	227989.13
1F1	F1	35.07	2004	45023.93	270143.59
1G1	G1	30.20	2005	45860.27	229301.36

1G2	G2	48.11	2005	63970.08	319850.41
1H3	H3	50.66	2005	64577.63	322888.17
1K3	K3	8.75	1995	10725.15	160877.30
1L3	L3	10.61	1995	17432.42	261486.35
1L4	L4	11.79	1995	20261.00	303915.01
1L5	L5	10.56	1995	30186.89	452803.31
1M2	M2	11.75	1996	15101.61	211422.52
1M3	M3	10.43	1995	11518.59	172778.87
1M4	M4	7.65	1995	12733.36	191000.39
1M6	M6	10.40	1995	18432.47	276487.12
1M7	M7	9.15	1995	15683.66	235254.93
1N1	N1	3.74	1996	12443.69	174211.62
1O8	O8	12.36	1995	24514.83	367722.52
1P2	P2	1.26	1996	12437.57	174126.04
1R2	R2	13.30	1996	21780.61	304928.55
1R1	R1	8.58	1997	11982.78	155776.11
1V1	V1	7.52	2005	15439.73	77198.64

Appendix 2: Dry rubber content fraction values obtained from GREL (2016)

GREL DRC VALUES 2016																							
DATE	DRC	DATE	DRC	DATE	DRC	DATE	DRC	DATE	DRC	DATE	DRC	DATE	DRC	DATE	DRC	DATE	DRC	DATE	DRC	DATE	DRC	DATE	DRC
1-Jan	-	27-Jan	62.8	22-Feb	59.2	19-Mar	56.8	14-Apr	62.2	10-May	60.2	5-Jun	59.0	1-Jul	57.5	27-Jul	59.2	22-Aug	58.5	17-Sep	62.8	13-Oct	63.1
2-Jan	62.8	28-Jan	62.0	23-Feb	61.8	20-Mar	-	15-Apr	64.9	11-May	59.2	6-Jun	59.7	2-Jul	59.9	28-Jul	56.2	23-Aug	64.8	18-Sep	60.3	14-Oct	62.2
3-Jan	-	29-Jan	64.6	24-Feb	60.9	21-Mar	59.8	16-Apr	59.3	12-May	60.4	7-Jun	60.9	3-Jul	60.0	29-Jul	54.0	24-Aug	65.1	19-Sep	65.8	15-Oct	61.3
4-Jan	58.1	30-Jan	55.8	25-Feb	62.7	22-Mar	58.9	17-Apr	-	13-May	62.7	8-Jun	56.3	4-Jul	62.6	30-Jul	64.9	25-Aug	66.1	20-Sep	61.6	16-Oct	63.8
5-Jan	56.8	31-Jan	57.4	26-Feb	59.5	23-Mar	58.6	18-Apr	59.4	14-May	60.1	9-Jun	62.0	5-Jul	61.0	31-Jul	58.7	26-Aug	62.2	21-Sep	65.6	17-Oct	57.6
6-Jan	61.0	1-Feb	61.8	27-Feb	61.4	24-Mar	-	19-Apr	61.0	15-May	59.2	10-Jun	58.5	6-Jul	57.2	1-Aug	60.0	27-Aug	57.6	22-Sep	62.9	18-Oct	56.5
7-Jan	59.1	2-Feb	57.8	28-Feb	-	25-Mar	-	20-Apr	64.1	16-May	62.1	11-Jun	62.6	7-Jul	59.4	2-Aug	55.1	28-Aug	59.3	23-Sep	56.2	19-Oct	60.0
8-Jan	58.1	3-Feb	58.0	29-Feb	59.8	26-Mar	-	21-Apr	61.2	17-May	60.0	12-Jun	58.6	8-Jul	-	3-Aug	63.5	29-Aug	63.1	24-Sep	62.9	20-Oct	61.7
9-Jan	62.5	4-Feb	59.7	1-Mar	63.1	27-Mar	-	22-Apr	66.2	18-May	52.9	13-Jun	58.0	9-Jul	-	4-Aug	60.9	30-Aug	63.2	25-Sep	59.8	21-Oct	59.6
10-Jan	60.4	5-Feb	60.7	2-Mar	58.5	28-Mar	-	23-Apr	66.8	19-May	60.0	14-Jun	58.3	10-Jul	62.4	5-Aug	62.4	31-Aug	59.4	26-Sep	58.1	22-Oct	61.9
11-Jan	61.8	6-Feb	60.6	3-Mar	60.0	29-Mar	62.2	24-Apr	-	20-May	62.5	15-Jun	57.9	11-Jul	58.6	6-Aug	56.6	1-Sep	66.3	27-Sep	59.8	23-Oct	60.4
12-Jan	60.1	7-Feb	64.8	4-Mar	61.9	30-Mar	60.8	25-Apr	60.5	21-May	60.7	16-Jun	58.0	12-Jul	56.5	7-Aug	61.0	2-Sep	57.9	28-Sep	56.9	24-Oct	60.4
13-Jan	55.7	8-Feb	59.4	5-Mar	58.9	31-Mar	62.2	26-Apr	64.3	22-May	61.4	17-Jun	57.8	13-Jul	58.5	8-Aug	59.1	3-Sep	57.2	29-Sep	57.7	25-Oct	56.6
14-Jan	61.4	9-Feb	62.5	6-Mar	-	1-Apr	60.8	27-Apr	59.6	23-May	58.6	18-Jun	58.9	14-Jul	58.2	9-Aug	61.3	4-Sep	57.5	30-Sep	56.8	26-Oct	59.4
15-Jan	62.9	10-Feb	62.4	7-Mar	-	2-Apr	63.9	28-Apr	60.5	24-May	61.0	19-Jun	55.7	15-Jul	-	10-Aug	58.5	5-Sep	59.9	1-Oct	63.4	27-Oct	57.4
16-Jan	59.4	11-Feb	65.6	8-Mar	60.7	3-Apr	-	29-Apr	62.6	25-May	61.3	20-Jun	61.6	16-Jul	58.7	11-Aug	59.3	6-Sep	55.8	2-Oct	63.4	28-Oct	58.7
17-Jan	62.9	12-Feb	62.7	9-Mar	60.4	4-Apr	59.4	30-Apr	59.5	26-May	55.7	21-Jun	60.2	17-Jul	54.3	12-Aug	58.1	7-Sep	55.8	3-Oct	63.1	29-Oct	58.3
18-Jan	60.0	13-Feb	64.2	10-Mar	62.2	5-Apr	61.3	1-May		27-May	64.9	22-Jun	55.2	18-Jul	64.5	13-Aug	61.9	8-Sep	58.2	4-Oct	57.7	30-Oct	60.9
19-Jan	61.3	14-Feb	63.8	11-Mar	-	6-Apr	57.5	2-May	62.7	28-May	63.2	23-Jun	59.6	19-Jul	63.4	14-Aug	59.9	9-Sep	65.2	5-Oct	57.6	31-Oct	59.5
20-Jan	59.9	15-Feb	63.0	12-Mar	64.5	7-Apr	61.3	3-May	58.5	29-May	65.1	24-Jun	62.6	20-Jul	62.0	15-Aug	55.8	10-Sep	65.3	6-Oct	62.6	1-Nov	59.2
21-Jan	61.6	16-Feb	63.6	13-Mar	-	8-Apr	63.9	4-May	59.7	30-May	62.1	25-Jun	64.6	21-Jul	56.4	16-Aug	56.8	11-Sep	62.8	7-Oct	56.9		
22-Jan	63.5	17-Feb	62.9	14-Mar	-	9-Apr	64.8	5-May	63.4	31-May	55.9	26-Jun	58.2	22-Jul	66.7	17-Aug	57.8	12-Sep	61.3	8-Oct	59.0		
23-Jan	62.5	18-Feb	55.7	15-Mar	62.0	10-Apr	-	6-May	60.7	1-Jun	58.4	27-Jun	60.9	23-Jul	61.3	18-Aug	53.6	13-Sep	63.9	9-Oct	59.4		
24-Jan	62.7	19-Feb	64.2	16-Mar	55.3	11-Apr	60.0	7-May	58.1	2-Jun	60.5	28-Jun	57.5	24-Jul	60.8	19-Aug	58.4	14-Sep	58.4	10-Oct	60.4		
25-Jan	58.1	20-Feb	59.5	17-Mar	60.4	12-Apr	62.4	8-May	63.4	3-Jun	61.6	29-Jun	58.1	25-Jul	59.5	20-Aug	60.1	15-Sep	64.2	11-Oct	59.3		
26-Jan	58.5	21-Feb	61.6	18-Mar	57.7	13-Apr	60.3	9-May	62.8	4-Jun	59.8	30-Jun	59.8	26-Jul	56.3	21-Aug	58.2	16-Sep	61.5	12-Oct	58.3		

Appendix 3: Google earth image metadata

Source	Google Maps Satellite
Projection	UTM
Datum	WGS 84 zone 30N
Date	15/01/2011
Altitude	NA
Aerial platform and orbit type	NA
Band wavelength	RGB
Date flown	NA
Flying speed	NA
Image Corrections	NA
Format	TIF
Spatial Resolution	30cm
Pixel Depth	32 bit
Uncompressed Size	5.8 GB
Sensor	NA

Appendix 4: Sample points data

Plot	Age (years)	Block	Trees	Total Trees per age	Area (Ha)	Total Area (Ha)
1	22	K5	24	49	13.5	25.2
2		K6	25		11.7	
3	21	K4	22	109	11.1	70.7
4		N4	23		15.3	
5		N7	22		14.2	
6		O3	18		15.2	
7		O5	24		14.9	
8	20	O2	23	106	11.3	64
9		P4	21		14.1	
10		P8	19		9.9	
11		R4	21		13.7	
12		M1	22		14.6	
13	19	Q1	17	60	8.3	26.1
14		R1	19		8.6	
15		S4	24		9.2	
16	17	T5	21	44	11.9	16.9
17		T6	23		5	
18	12	E2	23	73	30.7	97.9
19		E5	25		32.1	
20		F1	25		35.1	
21	11	G2	22	88	48.1	196.3
22		G3	22		26.6	
23		H1	23		70.9	
24		H3	21		50.7	
25	9	P1	25	25	34.7	34.7

Appendix 5: Field data collection sheet

Data Sheets for Field Data			
Coordinates			
Plot Number			
Date			
Stand Age			
Plot Area (m2)			
Planting Intensity			
Latex tappings per annum			
Per Unit Weight of Latex			
Number of Trees/Plot	**DBH_{170}**	**CPA**	**DRC**

Appendix 6: Latex carbon computation

Age	Block	Plot No	Area (Ha)	Latex (kg)	Latex Carbon (kg C per 500m²)	Latex Carbon (t C per 500m²)	Latex Carbon (t C ha⁻¹)
22	K6	1	11.71	387128.97	878.59	0.88	17.57
	K5	2	13.48	434811.15	857.24	0.86	17.14
21	K4	3	11.13	277343.04	662.23	0.66	13.24
	N4	4	15.34	388348.70	672.80	0.67	13.46
	N7	5	14.16	366484.14	687.83	0.69	13.76
	O3	6	15.21	438901.33	766.88	0.77	15.34
	O5	7	14.93	461358.83	821.24	0.82	16.42
20	P4	8	14.12	407351.24	766.70	0.77	15.33
	P8	9	9.88	215428.90	579.48	0.58	11.59
	O2	10	11.29	204144.42	480.54	0.48	9.61
	R4	11	13.65	340976.38	663.87	0.66	13.28
	M1	12	14.59	309261.58	563.33	0.56	11.27
19	Q1	13	8.26	122589.97	394.43	0.39	7.89
	S4	14	9.2	133040.83	384.31	0.38	7.69
	R1	15	8.58	155776.11	482.51	0.48	9.65
17	T5	16	11.93	191319.70	426.20	0.43	8.52
	T6	17	5.01	74746.95	396.50	0.40	7.93
12	E2	18	30.71	227989.13	197.30	0.20	3.95
	E5	19	32.08	306011.77	253.51	0.25	5.07
	F1	20	35.01	270143.59	205.07	0.21	4.10
11	G2	21	48.11	319850.41	176.69	0.18	3.53
	G3	22	26.63	175552.03	175.20	0.18	3.50
	H1	23	70.86	555532.23	208.35	0.21	4.17
	H3	24	50.66	322888.17	169.39	0.17	3.39
9	P1	25	34.74	135805.53	103.9	0.10	2.08

Appendix 7: Computation of aboveground and belowground carbon

Age	Block	Plot No.	Area (ha)	No. of Trees	Mean DBH_{170} (cm)	Mean C_{170} (cm)	Foliage (kg C per tree)	Stem (kg C per tree)	AGC (kg C per $500m^2$)	BGC (kg C per $500m^2$)	AGC ($t\ C\ ha^{-1}$)	BGC ($t\ C\ ha^{-1}$)
22	K6	1	11.71	4881	23.5	73.7	6.47	186.52	4824.77	530.24	96.5	10.6
	K5	2	13.48	5246	28.2	88.5	9.1	317.34	7834.42	717.01	156.69	14.3
21	K4	3	11.13	3498	28.7	90.2	9.42	335.15	7580.41	680.8	151.61	13.6
	N4	4	15.34	4811	22.9	72.1	6.2	174.46	4155.25	467.25	83.11	9.3
	N7	5	14.16	5665	23.6	74.1	6.54	189.53	4313.61	471.46	86.27	9.4
	O3	6	15.21	5027	22.9	72	6.2	174.31	3068.71	345.17	61.37	6.9
	O5	7	14.93	5687	23.8	74.8	6.66	194.83	4835.64	523.54	96.71	10.5
20	P4	8	14.12	6273	22.6	71	6.03	167.04	3634.47	414.83	72.69	8.3
	P8	9	9.88	3787	24.9	78.3	7.24	222.01	4355.73	450.87	87.11	9.0
	O2	10	11.29	2943	25	78.6	7.29	224.74	5336.78	550.11	106.74	11.0
	R4	11	13.65	5719	24.6	77.2	7.06	213.33	4628.02	485.68	92.56	9.7
	M1	12	14.59	4521	25.9	81.4	7.77	248.17	5630.7	560.93	112.61	11.2
19	Q1	13	8.26	2052	23.4	73.4	6.42	184.23	3241.13	357.71	64.82	7.2
	S4	14	9.2	2860	23.9	75.1	6.7	196.81	4884.33	526.97	97.69	10.5
	R1	15	8.58	2588	23.5	73.7	6.47	186.44	3665.41	402.88	73.31	8.1
17	T5	16	11.93	4774	22	69.2	5.75	154.87	3372.94	395.09	67.46	7.9
	T6	17	5.01	1894	21.3	66.9	5.4	140.39	3353.1	406.18	67.06	8.1
12	E2	18	30.71	13244	21.1	66.4	5.33	137.49	3284.87	400.76	65.7	8.0
	E5	19	32.08	15056	19.7	61.9	4.68	112.43	2927.97	382.62	58.56	7.7
	F1	20	35.01	14818	19.9	62.6	4.78	116.05	3020.73	390.51	60.41	7.8
11	G2	21	48.11	21981	19.9	62.5	4.76	115.28	2640.86	342.17	52.82	6.8
	G3	22	26.63	12352	21.1	66.2	5.3	136.51	3261.69	398.91	65.23	8.0
	H1	23	70.86	33731	19.6	61.5	4.63	110.21	2641.23	347.51	52.82	7.0
	H3	24	50.66	22448	19.2	60.2	4.44	103.35	2263.62	304.42	45.27	6.1
9	P1	25	34.74	13718	17	53.3	3.54	72.61	1903.8	288.64	38.08	5.8

Appendix 8: Normality test for differences in carbon content of latex for different ages

Tests of Normality

	Kolmogorov-Smirnov[a]			Shapiro-Wilk		
	Statistic	df	Sig.	Statistic	df	Sig.
LC t C ha^{-1}	0.142	25	0.200*	0.928	25	0.079

*. This is a lower bound of the true significance.
a. Lilliefors Significance Correction

Appendix 9: One-way ANOVA test for differences in carbon content of latex for different ages

ANOVA

LC t C ha-1

	Sum of Squares	df	Mean Square	F	Sig.
Between Groups	560.071	7	80.010	45.028	.000
Within Groups	30.207	17	1.777		
Total	590.279	24			

Appendix 10: Post-hoc multi-comparison test

Pairwise Comparisons						
Dependent Variable: LC t C ha-1						
					95% Confidence Interval for Difference[b]	
(I) AGE		Mean Difference (I-J)	Std. Error	Sig.[b]	Lower Bound	Upper Bound
22	21	2.911	1.115	.512	-1.213	7.035
	20	5.139*	1.115	.007	1.015	9.263
	19	8.945*	1.217	.000	4.445	13.445
	17	9.130*	1.333	.000	4.201	14.059
	12	12.982*	1.217	.000	8.482	17.482
	11	13.708*	1.154	.000	9.439	17.976
	9	15.275*	1.633	.000	9.238	21.312
21	22	-2.911	1.115	.512	-7.035	1.213
	20	2.228	.843	.479	-.890	5.346
	19	6.034*	.973	.000	2.434	9.634
	17	6.219*	1.115	.001	2.095	10.343
	12	10.071*	.973	.000	6.471	13.671
	11	10.797*	.894	.000	7.490	14.103
	9	12.364*	1.460	.000	6.964	17.764
20	22	-5.139*	1.115	.007	-9.263	-1.015
	21	-2.228	.843	.479	-5.346	.890
	19	3.806*	.973	.032	.206	7.406
	17	3.991	1.115	.065	-.133	8.115
	12	7.843*	.973	.000	4.243	11.443
	11	8.568*	.894	.000	5.262	11.875
	9	10.136*	1.460	.000	4.736	15.536
19	22	-8.945*	1.217	.000	-13.445	-4.445
	21	-6.034*	.973	.000	-9.634	-2.434
	20	-3.806*	.973	.032	-7.406	-.206
	17	.185	1.217	1.000	-4.315	4.685
	12	4.037*	1.088	.049	.012	8.062
	11	4.763*	1.018	.006	.998	8.527
	9	6.330*	1.539	.020	.638	12.022
17	22	-9.130*	1.333	.000	-14.059	-4.201
	21	-6.219*	1.115	.001	-10.343	-2.095
	20	-3.991	1.115	.065	-8.115	.133
	19	-.185	1.217	1.000	-4.685	4.315
	12	3.852	1.217	.158	-.648	8.352
	11	4.577*	1.154	.028	.309	8.846
	9	6.145*	1.633	.043	.108	12.182
12	22	-12.982*	1.217	.000	-17.482	-8.482
	21	-10.071*	.973	.000	-13.671	-6.471
	20	-7.843*	.973	.000	-11.443	-4.243

	19	-4.037*	1.088	.049	-8.062	-.012
	17	-3.852	1.217	.158	-8.352	.648
	11	.726	1.018	1.000	-3.039	4.491
	9	2.293	1.539	1.000	-3.399	7.985
11	22	-13.708*	1.154	.000	-17.976	-9.439
	21	-10.797*	.894	.000	-14.103	-7.490
	20	-8.568*	.894	.000	-11.875	-5.262
	19	-4.763*	1.018	.006	-8.527	-.998
	17	-4.577*	1.154	.028	-8.846	-.309
	12	-.726	1.018	1.000	-4.491	3.039
	9	1.568	1.490	1.000	-3.944	7.079
9	22	-15.275*	1.633	.000	-21.312	-9.238
	21	-12.364*	1.460	.000	-17.764	-6.964
	20	-10.136*	1.460	.000	-15.536	-4.736
	19	-6.330*	1.539	.020	-12.022	-.638
	17	-6.145*	1.633	.043	-12.182	-.108
	12	-2.293	1.539	1.000	-7.985	3.399
	11	-1.568	1.490	1.000	-7.079	3.944

Based on estimated marginal means

*. The mean difference is significant at the .05 level.

b. Adjustment for multiple comparisons: Bonferroni.

Appendix 11: Descriptive statistics of diameter at breast height

Descriptive Statistics for Diameter at Breast Height of 170cm (DBH170)

Age of tree		N	Mean	Minimum	Maximum	Range	Std. Deviation	Std. Error of Mean	Variance	Skewness	Std. Error of Skewness	Kurtosis	Std. Error of Kurtosis
22	K6	25	23.470	5.6	39.8	34.2	7.4163	1.4833	55.001	-.432	.464	.693	.902
	K5	24	28.183	16.3	40.9	24.6	6.6530	1.3580	44.262	.060	.472	-.562	.918
21	K4	22	28.718	20.8	33.5	12.7	3.1129	.6637	9.690	-.644	.491	.405	.953
	N4	23	22.936	13.6	29.3	15.7	4.1379	.8628	17.122	-.653	.481	-.351	.935
	N7	22	23.600	18.0	29.6	11.6	3.7016	.7892	13.702	-.008	.491	-1.390	.953
	O3	17	22.929	17.6	28.8	11.2	3.2365	.7850	10.475	.090	.550	-.208	1.063
	O5	24	23.825	17.1	30.5	13.4	4.0756	.8319	16.611	.097	.472	-1.125	.918
20	P4	21	22.595	15.6	25.7	10.1	2.7229	.5942	7.414	-.970	.501	.847	.972
	P8	19	24.921	19.3	30.3	11.0	2.4600	.5644	6.052	-.328	.524	1.125	1.014
	O2	23	25.026	15.4	32.8	17.4	4.4600	.9300	19.892	-.185	.481	.334	.935
	R4	21	24.581	18.1	31.7	13.6	3.8147	.8324	14.552	.268	.501	-.594	.972
	M1	22	25.895	19.7	31.8	12.1	3.1103	.6631	9.674	-.281	.491	.247	.953
19	Q1	17	23.371	17.3	34.8	17.5	4.6879	1.1370	21.976	1.055	.550	.692	1.063
	S4	24	23.908	15.3	28.9	13.6	3.9637	.8091	15.711	-.637	.472	-.524	.918
	R1	19	23.467	16.5	29.7	13.2	3.4850	.7995	12.145	-.210	.524	-.563	1.014
17	T5	21	22.014	15.8	27.5	11.7	2.8370	.6191	8.048	-.137	.501	-.236	.972
	T6	23	21.283	15.5	28.3	12.8	3.5561	.7415	12.646	.532	.481	-.464	.935
12	E2	23	21.130	16.8	25.9	9.1	2.1933	.4573	4.810	.047	.481	-.455	.935
	E5	25	19.716	15.8	24.3	8.5	2.6769	.5354	7.166	.281	.464	-1.279	.902
	F1	25	19.932	15.2	23.8	8.6	2.2058	.4412	4.866	-.371	.464	-.340	.902
11	G2	22	19.886	16.4	23.6	7.2	2.0030	.4270	4.012	.119	.491	-.691	.953
	G3	23	21.078	16.3	27.2	10.9	2.6778	.5584	7.171	.153	.481	-.142	.935
	H1	23	19.581	15.8	23.4	7.6	2.1957	.4578	4.821	-.241	.481	-.960	.935
	H3	21	19.152	15.3	22.9	7.6	1.8408	.4017	3.389	.055	.501	.208	.972
9	P1	25	16.960	13.4	19.9	6.5	1.9744	.3949	3.898	-.212	.464	-1.074	.902
	Total	554											

Appendix 12: Normality test for carbon pools

Tests of Normality

Kolmogorov-Smirnov[a]		Shapiro-Wilk		
Statistic	Sig.	Statistic	df	Sig.
0.325	0.000	0.748	75	0.000

a. Lilliefors Significance Correction

Appendix 13: Kruskal Wallis test of significant differences among the carbon pools

Carbon content (t C ha^{-1})		N	Mean Rank	Test Statistic	
				Chi-square (df)	P-value
Carbon Pools	Aboveground Carbon	25	63	49.436 (2)	0.000
	Latex Carbon	25	26.44		
	Belowground carbon	25	24.56		
	Total	75			

Appendix 14: Kruskal Wallis multi-comparison test of differences

Paired Comparison	**N**	**Mean Ranks**	**Kruskal Wallis**		**Effect Size (r)**
Carbon Pools			Chi-Squared (df)	p-value	
AGC	25	38	36.766 (1)	0.000	0.750
BGC	25	13			
Total	50				
AGC	25	38	36.766 (1)	0.000	0.750
Latex	25	13			
Total	50				
Latex	25	26.44	0.208 (1)	0.648	0.004
BGC	25	24.56			
Total	50				

Effect size = Chi-Squared/Total N-1(Green & Salkind, 2008)